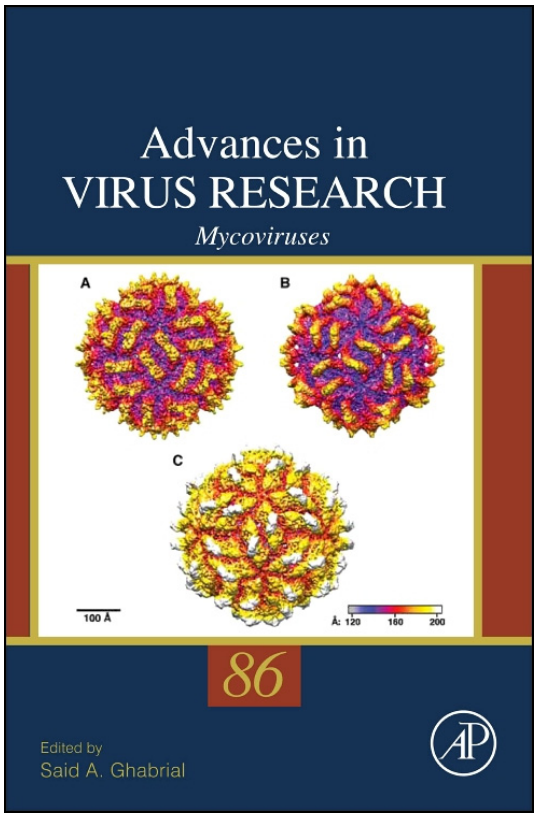

From: Said A. Ghabrial, Sarah E. Dunn, Hua Li, Jiatao Xie and Timothy S. Baker, Viruses of *Helminthosporium (Cochlioblus) victoriae*. In Said A. Ghabrial, editor: *Advances in Virus Research,* Vol. 86, Burlington: Academic Press, 2013, pp. 289-325.
ISBN: 978-0-12-394315-6

CHAPTER ELEVEN

Viruses of *Helminthosporium* (*Cochlioblus*) *victoriae*

Said A. Ghabrial[*,1], Sarah E. Dunn[†], Hua Li[*], Jiatao Xie[*] and Timothy S. Baker[‡]

[*]Department of Plant Pathology, University of Kentucky, Lexington, Kentucky, USA
[†]Department of Chemistry and Biochemistry, University of California, San Diego, La Jolla, California, USA
[‡]Department of Chemistry and Biochemistry, and Division of Biological Sciences, University of California, San Diego, La Jolla, California, USA
[1]Corresponding author: e-mail address: saghab00@email.uky.edu

Contents

Abstract

The enigma of the transmissible disease of *Helminthosporium victoriae* has almost been resolved. Diseased isolates are doubly infected with two distinct viruses, the victorivirus Helminthosporium victoriae virus 190S and the chrysovirus HvV145S. Mixed infection, however, is not required for disease development. DNA transformation experiments and transfection assays using purified HvV190S virions strongly indicate that HvV190S alone is necessary for inducing disease symptoms. HvV145, like other chrysoviruses, appears to have no effect on colony morphology. This chapter will discuss the molecular biology of the two viruses and summarize recent results of characterization of host gene products upregulated by virus infection. Furthermore, the novel structural features of HvV190S capsid will be highlighted.

Advances in Virus Research, Volume 86
ISSN 0065-3527
http://dx.doi.org/10.1016/B978-0-12-394315-6.00011-8

1. INTRODUCTION

The senior author of this chapter has written several reviews in the past on the viruses that infect the plant pathogenic fungus *Helminthosporium* (*Cochlioblus*) *victoriae*. However, this review is special because it is the last that he will write. In this review, we would like to reflect on the times and people who were involved and most importantly the accomplishments: how much we do know about the *H. victoriae* system since 1959 when the first report on the transmissible disease of *H. victoriae* was published (Lindberg, 1959).

As a virology graduate student (1961–1965) at the Plant Pathology Department, Louisiana State University (LSU), the senior author was intrigued by the etiology of the transmissible disease of *H. victoriae* and by the pathotoxin "victorin," a cyclized pentapeptide of 814 Da (Wolpert et al., 1985) which is produced by virulent isolates of *H. victoriae*. The findings that victorin reproduces the disease symptoms in the absence of the fungus and that cell-free, fungal culture filtrate diluted one million-fold was not only toxic but also exhibited the same specificity toward oat genotypes as the fungus (Meehan & Murphy, 1947) were of considerable interest. During his tenure at LSU, Professors G. D. Lindberg and H. E. Wheeler were directing nationally recognized research programs on the transmissible disease of *H. victoriae* and mode of action of victorin, respectively. Nevertheless, the senior author did his research on another fascinating project dealing with the physiological basis of the virus-induced Tabasco pepper wilt. With some insight from Professor Wheeler's research on the effect of victorin treatment on membrane permeability and $K+$ efflux resulting in severe wilt of oat leaves (Wheeler & Black, 1962), my studies determined that changes in membrane permeability and $K+$ efflux were key events in the wilt syndrome of virus-infected Tabasco pepper (Ghabrial & Pirone, 1967).

The interest in the *H. victoriae* system was rekindled when he joined the Plant Pathology Department at the University of Kentucky (UK) in 1972 as an Assistant Professor. Luckily, Professor Wheeler had moved earlier to UK from LSU and supplied him with various normal and abnormal isolates of *H. victoriae*. Because of lack of funding for fungal virus projects in the 1970s and 1980s, the *H. victoriae* project was secondary to his plant virus research responsibilities. The objectives at the initiation of studies on viruses of *H. victoriae* in 1976 were to address the following three questions:

i. Are viruses associated with the disease phenotype? If so, then isolate the viruses involved and characterize them at the biochemical and molecular levels.
ii. What is the evidence for virus etiology of the transmissible disease of *H. victoriae*?
iii. Is virus infection required for vectorin production? Or does virus infection alter victorin production and thus virulence of *H. victoriae* isolates?

The answers to these questions and more are listed among the highlights of our journey with *H. victoria* viruses under Section 2.

2. HISTORICAL PERSPECTIVES

H. victoriae was first described in 1946 as the causal agent of a new disease in oats called Victoria blight, named after the parent cultivar, Victoria (Meehan & Murphy, 1946). The Victoria blight disease arose after the introduction of the *Pc-2* resistance gene to a completely different disease, crown rust of oats (causal agent: *Puccinia cronata*), which was genetically linked to susceptibility to a previously unknown soil fungus, *H. victoriae* (Litzenberger, 1949). The disease caused by *H. victoriae* rose to epidemic proportions in 1947 and 1948 and resulted in serious yield losses in most oat-growing regions of the United States (Litzenberger, 1949).

Although Victoria-derived oat cultivars were subsequently abandoned in the major oat-cropping areas, they continued to be grown in relatively large acreage in some of the Southern States during the 1950s (Lindberg, 1960; Scheffer & Nelson, 1967). The discovery in 1959 of a transmissible disease of *H. victoriae* was based on observed cultural abnormalities in isolates obtained from blighted "Victorgrain" oat plants in Louisiana (Lindberg, 1959). Lindberg observed that some of the *H. victoriae* colonies isolated from diseased oats were stunted and highly sectored. Following an initial period of normal growth, sectors appeared at the margins of the colonies with concomitant collapse of existing aerial mycelium and almost complete inhibition of colony expansion (Psarros and Lindberg, 1962). Lindberg referred to these abnormalities as a "disease" of the fungus and showed that the disease could be transmitted to normal colonies via hyphal anastomosis with diseased colonies. Since the fields of "Victorgrain" oats in Louisiana from which diseased and normal *H. victoriae* were isolated did not suffer significant yield losses, which was unusual for this serious disease of oats, it was suggested that a reduction in the pathogenicity level of *H. victoriae* had

occurred and that this might be attributed to the transmissible disease of the fungus.

Over 50 years ago, Lindberg suggested a viral role in the disease of *H. victoriae*, but it was the work in the senior author's laboratory in the late 1970s that presented evidence for virus involvement. Diseased isolates of *H. victoriae* have been found to contain two serologically and electrophoretically distinct viruses designated according to their sedimentation values as the 190S and 145S viruses (Ghabrial, Sanderlin, & Calvert, 1979; Sanderlin & Ghabrial, 1978). Further studies on these two viruses led to their molecular characterization and the creation of a new family of mycoviruses (*Chrysoviridae*) and a new genus (*Victorivirus*) in the family *Totiviridae*. In addition, some highlights of the *H. victoriae*-virus quest include

- First report of association of two distinct viruses (HvV190S and HvV145S) with diseased isolates of *H. victoriae* (Sanderlin & Ghabrial, 1978).
- Virulent fungal isolates known to be potent producers of victorin were found to be virus free. Thus, virus infection is not required for victorin production. Interestingly, virus-infected isolates produce little or no victorin and are hypovirulent (Ghabrial, 1986).
- Discovery of HvV190S capsid protein (CP) heterogeneity as a consequence of posttranslational modification (phosphorylation and proteolytic processing) and the occurrence of two types of particles that differ in capsid composition and phosphorylation state (Ghabrial, Bibb, Price, Havens, & Lesnaw, 1987; Ghabrial & Havens, 1989, 1992).
- HvV190S was the first totivirus infecting a filamentous fungus to be characterized at the molecular level. HvV190S was the only virus from filamentous fungi that is listed as a member of *Totiviridae* (Huang & Ghabrial, 1996).
- Molecular characterization of HvV190S (Huang & Ghabrial, 1996) and elucidation of the expression strategy (stop-restart) of its RNA-dependent RNA polymerase (RdRp) led to the realization that many HvV190S-like viruses that infect filamentous fungi should be grouped together in a separate genus (*Victorivirus*; derived from the species name of the host, *H. victoriae*; Ghabrial & Nibert, 2009; Li, Havens, Nibert, & Ghabrial, 2011).
- Established that Penicillium chrysogenum virus (PcV), like HvV145S, has a quadripartite genome. This ended the confusion about the taxonomic status of PcV and HvV145S, and helped to create the new family *Chrysoviridae* for mycoviruses with quadripartite genomes (Jiang &

Ghabrial, 2004). Identification and molecular characterization of host gene products that are upregulated by virus infection (e.g., the multifunctional protein Hv-p68 with alcohol oxidase/protein kinase/RNA-binding activities and the antifungal preproprotein victoriocin; de Sá, Havens, & Ghabrial, 2010; Soldevila & Ghabrial, 2001).
- Presented evidence in support of a viral etiology of the disease of *H. victoriae* (Ghabrial, 2008b; Li, Havens, & Ghabrial, 2013).
- Collaboration with structure biology laboratories revealed novel capsid structural features of mycoviruses (this chapter, Chapters 3 and 4, this volume). This was made possible because of the ability to purify well-characterized victoriviruses and chrysoviruses (e.g., HvV190S and PcV as well as selected partitiviruses) in good quantity and high quality.

3. VIRUSES OF *H. VICTORIAE*

3.1. Helminthosporium victoriae virus 190S (HvV190S)—genus *Victorivirus*, family *Totiviridae*

Like the majority of members of *Totiviridae*, the nonsegmented HvV190S dsRNA genome comprises two large overlapping open reading frames (ORFs). The 5′ proximal ORF (ORF 1) codes for the CP, whereas the 3′ ORF (ORF 2), which is in the −1 frame relative to ORF 1, encodes the RdRp (Fig. 11.1) with its characteristic eight conserved motifs (Huang & Ghabrial, 1996). Several lines of evidence (Huang & Ghabrial, 1996) indicate that translation of ORF1 starts at the AUG at position 290. This initiation codon, however, resides in an unfavorable sequence context (UCCAUGU). The 5′ end of the positive strand of the dsRNA genome is uncapped and highly structured and contains a relatively long (289 nt) 5′ untranslated region (5′ UTR). These structural features of the 5′ UTR of HvV190S positive sense RNA predict that the CP ORF (with its AUG present in suboptimal context) is possibly translated via a cap-independent mechanism. Site-directed mutagenesis verified that the stop codon (UGA) at position 2606–2608 is the authentic termination codon for the CP ORF (Huang & Ghabrial, 1996; Huang, Soldevila, Webb, & Ghabrial, 1997). The downstream ORF of the HvV190 dsRNA genome, which encodes the RdRp, is in a −1 frame with respect to the CP ORF and its translational start codon (nt positions 2605–2607) overlaps the stop codon for the upstream CP ORF (nt positions 2606–2608) in the tetranucleotide sequence 2605-AUGA-2608 (Fig. 11.1A).

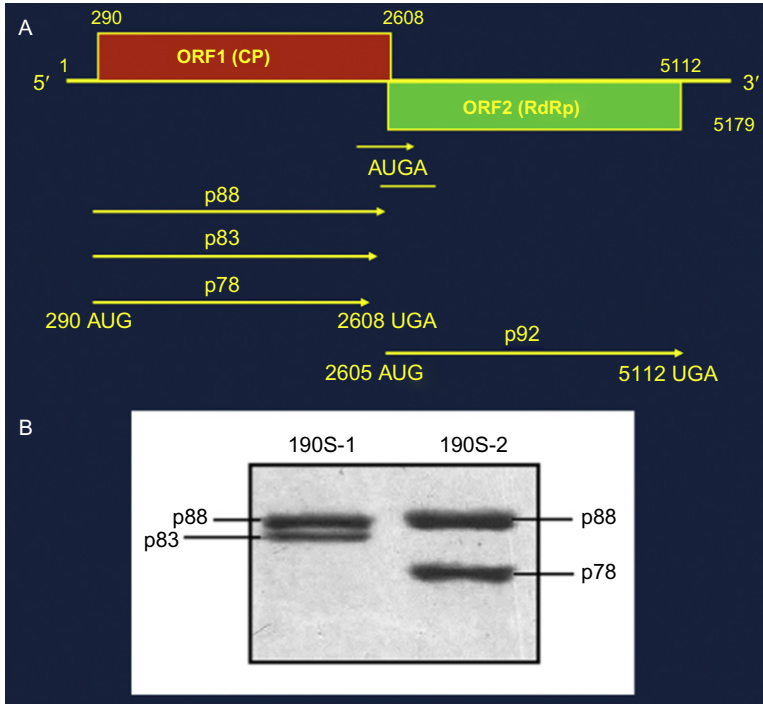

Figure 11.1 (A) Genome organization of Helminthosporium victoriae 190S virus, the type species of the newly recognized genus *Victorivirus*. The dsRNA genome encompasses two large overlapping ORFs with the 5′ ORF encoding a capsid protein (CP) and the 3′ ORF encoding an RNA-dependent RNA polymerase (RdRp). Note that the termination codon of the CP ORF overlaps the initiation codon of the RdRp ORF in the tetranucleotide sequence AUGA. Although the capsid is encoded by a single gene, three related polypeptides (p88, p83, and p78) are resolved by SDS-PAGE of purified virions. Whereas p88 is the primary translation product, p83 and p78 are generated via proteolytic processing of p88 at its C-terminus. (B) Two types of particles (190S-1 and 190S-2) that differ slightly in sedimentation and capsid composition are resolved by sucrose density gradient centrifugation of virion preparations. The 190S-1 capsids contain p88 and p83, occurring in approximately equimolar amounts, and the 190S-2 capsids comprise similar amounts of p88 and p78. The capsids p88 and p83 are phosphoproteins, whereas p78 is nonphosphorylated (Ghabrial & Havens, 1992).

Although a single gene encodes the capsid of Hv190SV like other totiviruses, the HvV190S capsid comprises two closely related major CPs, either p88 and p83 or p88 and p78 (Fig. 11.1). Whereas p88 is the primary translation product of ORF1, p83 and p78 are C-terminally cleaved forms of p88, which are virion associated but are not required for capsid assembly (Soldevila, Huang, & Ghabrial, 1998). Capsid heterogeneity and

posttranslational modification of the primary translation product may be a common feature of victoriviruses (Nomura, Osahki, Iwanami, Matsumoto, & Ohtsu, 2003). Purified HvV190S virion preparations contain two types of particles, 190S-1 and 190S-2, which differ slightly in sedimentation rates (190S-1 is resolved as a shoulder on the slightly faster sedimenting component 190S-2) and capsid composition (Fig. 11.1B). The 190S-1 capsids contain p88 and p83, occurring in approximately equimolar amounts, and the 190S-2 capsids comprise similar amounts of p88 and p78. Though p78 is non-phosphorylated, p88 and p83 are phosphoproteins (Ghabrial & Havens, 1992). Phosphorylation and proteolytic processing are proposed to play a role in the virus life cycle; phosphorylation of CP may be necessary for its interaction with viral nucleic acid and/or phosphorylation may regulate dsRNA transcription/replication. Phosphorylation/dephosphorylation may regulate viral dsRNA transcription; the finding that the more highly phosphorylated virions of the 190S-1 component were more efficient in transcriptase activity than those of the 190S-2 component is of interest in this regard (Ghabrial & Havens, 1992). Proteolytic processing and cleavage of a C-terminal peptide, which leads to dephosphorylation and the conversion of p88 to p78, may play a role in the release of the plus-strand RNA transcripts from virions (Ghabrial & Havens, 1992).

The overlap regions in the dsRNA genomes of the majority of victoriviruses (Fig. 11.2B) are of the AUGA type, where the initiation codon of the RdRp ORF overlaps the termination codon of the CP ORF. This suggests that the expression of RdRp occurs by a mechanism different from the translational frameshifting utilized by most viruses in the family *Totiviridae* to express their RdRps. It is of interest that the overlap region in one of the newly reported victoriviruses, BbRV1, is of the TAAUG type (with similarity to the overlap region in hypoviruses; Guo, Sun, Chiba, Araki, & Suzuki, 2009). There is no overlap region for another recently reported victorivirus, TcV1, as the CP stop codon and the RdRp initiation codon (TAAAUG) are positioned side by side with no spacer sequence (Herrero & Zabalgogeazcoa, 2011). The complete nucleotide sequences of Hv190SV and 13 other members and probable members of the genus *Victorivirus* have been reported and deposited in GenBank. The genomic, biochemical, and structural properties of HvV190S are the best characterized among all victoriviruses. The RdRp-encoding ORF 2 of HvV190S is expressed via a stop–restart (coupled termination–reinitiation) mechanism (Li et al., 2011; Soldevila & Ghabrial, 2000). The HvV190S RdRp is detectable as a separate, virion-associated component, consistent

A

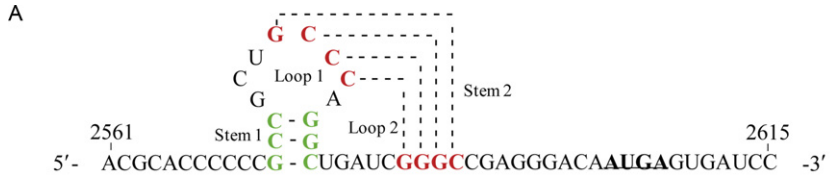

B

Virus	RNA Sequence	MFE
BbRV1	CCCTGTCGCAATTGCCGGTGCTGCCCCACCCGGAGGGCCGAACCCCGAGTAATGG	-14.0
BfTV1	UACCCCUCCGCGUUCCCCUGCUGCCCCAGGUAACGGGCCGGACACGAUAUGAGUG	-13.6
CeRV1	GUAGUAUCUUCUUCUGUGGCUGCCCCCACUAAUGAGGGCCGAAACGAUGUCUAGA	-14.3
CmRV	AGGUGGUGACGUUCACGGUGCCGCCGGAGCCUUACCGGCUCCACAAGUAUGAUCG	-16.0
EfV1	UCCUCCCAUGCCUGAGGCUGCCACCGGUGCCGAACCGGUGCCCCAAGCAUGAUUG	-21.4
GaRV-L1	CGCCCACCUGCCAGCCGAAGCUACUGCUGCUGAAGCAGUGCCCGCUCAAUGAUUG	-16.5
HmTV-17	GGCUGAAGCCAUGCAACAGGACGCAGCCCUGCAAGCUGCGGGGGCUCAAUGAAGG	-20.2
HvV190S	CAUCCACGCACCCCCCGCCGCUGCCCAGGCUGAUCGGGCCGAGGGACAAUGAGUG	-17.0
MoV1	AGGGCCGACCCCCGAACCCCACGGCGCGGCGCCUAGCCUGCACGAAUAGAUAUGG	-13.8
MoV2	AGGCAAUAACAACGAGCAGGCCGCCGGCGCCCAGCCGGCCCCCGCUCAAUGAUUG	-23.4
SsRV1	GCCCCCCCUGUAGCACCCGGCCCCGCCCAGCCUGACGGGCCCGCCAAUGAAUAAG	-16.2
TcV1	CACTGCTCCCCCTGTTGCCGACCCCCAGGCTATGGTGGGCGACCAGATCTAAATG	-16.6

Figure 11.2 (A) H-type pseudoknot predicted for stop–restart region of HvV190S. A predicted RNA pseudoknot structure is encoded near the 3′ end of ORF1 preceding the stop–restart site. The nucleotide positions are indicated, and the stop–restart site is in boldface and underlined. Dashed lines indicate base pairs predicted to form stem 1 (green) and stem 2 (red). (B) Sequences of HvV190S-like fungal viruses (victoriviruses) predicted to form a pseudoknot structure upstream of the stop and restart sites in each. Stem 1 (green) and stem 2 (red) are color coded to match panel A. Virus names and abbreviations: BbRV1, Beauveria bassiana RNA virus; BfTV1, Botryotinia fuckeliana totivirus 1; CeRV1, Chalara elegans RNA virus 1; CmRV, Coniothyrium minitans RNA virus; EfV1, Epichloe festucae virus 1; GaRV-L1, Gremmeniella abietina RNA virus L1; HmTV1–17, Helicobasidium mompa totivirus 1–17; HvV190S, Helminthosporium victoriae virus 190S; MoV1 and MoV2, Magnaporthe oryzae viruses 1 and 2; SsRV1, Sphaeropsis sapinea RNA virus 1 and TcV1, Tolypocladium cylindrosporum virus 1. MFE, minimum free energy value for structure prediction at 37°C.

with its independent translation from ORF 2. The tetranucleotide AUGA overlap region, or a very similar structure, is characteristic of the overlap region of all victoriviruses (Fig. 11.2B; Ghabrial & Nibert, 2009; Li et al., 2011). Termination–reinitiation primarily depends on a 32-nt stretch of RNA immediately upstream of the AUGA motif, including a predicted

pseudoknot structure (Fig. 11.2A). The close proximity by which this predicted structure is followed by the ORF 1 stop codon appears to be particularly important for promoting translation of the downstream ORF. Similar sequence motifs and predicted RNA structures in other victoriviruses suggest that they all share a related stop–restart strategy for RdRp translation (Fig. 11.2B). Members of genus *Victorivirus* thus provide unique opportunities for exploring molecular mechanisms of translational coupling. It is noteworthy that translation of the downstream RdRp of HvV190S via coupled termination–reinitiation represents the first example of this expression strategy to be identified in a dsRNA virus.

The finding that translation of the ORF 1 and termination at its stop codon are absolute requirements for reinitiation at the victorivirus RdRp start codon distinguishes this process from IRES-mediated initiation (Hellen & Sarnow, 2001), as well as from leaky scanning (Kozak, 2002) and ribosomal shunting (Ryabova & Hohn, 2000). Leaky scanning can be further ruled out as there are >20 AUG codons in reasonably favorable context upstream of the RdRp start codon. The fact that RdRp is expressed from its downstream start codon as a separate, nonfused protein also distinguishes this process from ribosomal frameshifting (Dinman, Icho, & Wickner, 1991) and in-frame read-through of termination codons (Dreher & Miller, 2006), which generate fusion proteins.

The stop–restart strategy for expressing the downstream RdRp ORF allows HvV190S to produce two separate proteins from a single mRNA. This strategy furthermore allows HvV190S to regulate the level of RdRp expression (lower) relative to CP expression (much higher), consistent with the fact that only one or two RdRp molecules are present in each HvV190S virion versus 120 CP molecules (Castón et al., 2006). It is reasonable to predict that the abundance of RdRp molecules must be regulated so that the appropriate copy number is available for proper virion assembly and competence for replication (Dinman & Wickner, 1992). Although it is not known how the plus-strand RNA of HvV190S is packaged into assembling progeny virions, it is thought by analogy to Saccharomyces cerevisiae virus L-A (ScV-L-A), the prototype of both genus *Totivirus* and family *Totiviridae*, that the RdRp, through its binding affinity for single-stranded RNA, would recruit the progeny plus-strand RNA to ensure its packaging into particles (Dinman & Wickner, 1992). The identification of a predicted pseudoknot as a key determinant of the stop–restart mechanism in HvV190S and other victoriviruses is exciting. The predicted pseudoknot must be located closely upstream of the CP stop codon (Li et al., 2011), presumably so that it can

tether the terminating ribosome or components thereof, which can then reinitiate with limited efficiency at the next downstream start codon (see Powell, Brown, & Brierley, 2008 for a review).

Among viral mRNAs, the mechanism of translational coupling has perhaps been best studied with feline calicivirus and rabbit hemorrhagic disease virus (Luttermann & Meyers, 2007; Meyers, 2007). In these viruses, 84–87 nt of RNA sequence immediately upstream of the overlapping stop–restart codons, termed the "termination upstream ribosome binding site" (TURBS), are required for efficient reinitiation (Luttermann & Meyers, 2007, 2009; Meyers, 2003, 2007). Two distinct regions (motifs 1 and 2) within the TURBS have been shown to play significant roles. Of these, motif 1 is more important because it is conserved among different caliciviruses and is complementary to a small, single-stranded region at the tip of helix 26 of 18S rRNA, which is juxtaposed to mRNA in the translating ribosome (Matassova, Venjaminova, & Karpova, 1998). This complementary region is thought to tether the mRNA to the 40S subunit, allowing time for the ribosome to acquire the initiation factors necessary for translation of the downstream ORF (Meyers, 2003, 2007). There is also evidence that the TURBS is involved in recruiting eukaryotic initiation factor 3 (eIF3) and eIF3/40S complexes (Pöyry et al., 2007). The multisubunit eIF3 complex plays multiple roles in translation initiation including dissociating the 60S and 40S ribosomal subunits after termination, and it is therefore possible that the TURBS is involved in both ribosome dissociation/recycling and 40S tethering (Powell et al., 2008).

The stop–restart strategy of HvV190S and other victoriviruses is in line with those for the other RNA viruses known to utilize this strategy. Of particular note among all of these viruses is the consistent importance of a region of sequences closely upstream of the stop and restart codons. Interestingly, in the case of victoriviruses, this region (32 nt in length) contains a predicted pseudoknot. Li et al. (2011) presented experimental (via mutational analysis) and genetic evidence for the importance of the predicted pseudoknot sequence in HvV190S. Present results, however, do not rule out a role for sequences upstream of the predicted pseudoknot in the translation of ORF 2. In other viral mRNAs, including ones from other members of the family *Totiviridae*, pseudoknots are known to be structural features that promote translation of an alternative ORF by −1 ribosomal frameshifting (Dinman et al., 1991; Wang, Yang, Shen, & Wang, 1993). Ribosomal pausing induced by the pseudoknot is thought to be important in at least some of those cases (Plant et al., 2003).

The possibility that the predicted pseudoknot sequence upstream of the stop and restart codons of HvV190S and other victoriviruses may interact with the host 18S rRNA was considered, given previous findings with caliciviruses and influenza B viruses (Luttermann & Meyers, 2007, 2009; Powell et al., 2008). Interestingly, a portion of loop 2 in the predicted pseudoknot of HvV190S (Fig. 11.2A) has the sequence CUGAUCG, which is complementary to nt positions 909–915 of the *Cochliobolus* (anamorph: *Helminthosporium*) *sativus* 18S rRNA (Schoch et al., 2006). However, (a) the HvV190S sequence CUGAUCG is not conserved among other victoriviruses (see Fig. 11.2B); (b) the identified region of *Cochliobolus* 18S rRNA does not align with the region of mammalian 18S rRNA implicated in the stop–restart mechanisms of caliciviruses and influenza B viruses; and (c) based on RNA folding predictions, the identified region of *Cochliobolus* 18S rRNA forms part of a stem, unlike the single-stranded region of mammalian 18S rRNA implicated in the stop–restart mechanisms of caliciviruses and influenza B viruses. Therefore, the role of the predicted pseudoknot structure in victoriviruses is likely not to promote base pairing with 18S rRNA. This possibility, however, cannot be ruled out.

The mechanism by which the predicted pseudoknot can bring about coupled translation of victoriviruses is not known. The nonpolyadenylated victorivirus mRNA with a stop codon in the middle of the molecule is reminiscent of a nonsense-containing mRNA without polyA binding protein (PABP) (Amrani et al., 2004). These authors showed that in the absence of PABP the ribosomes tend to remain bound to mRNA in the vicinity of the termination codon. We predict that the secondary structure of the victorivirus mRNA that is upstream of the CP stop codon is present to prevent terminating ribosomes from sliding backward on the mRNA, thus helping to reposition them on the RdRp initiation codon. Although this is an attractive model, the HvV190S mRNA derived from transformants in our experimental system is predicted to be polyadenylated. Furthermore, the required close proximity of the predicted pseudoknot to the CP stop codon would interfere with the reformation of the predicted pseudoknot, particularly stem 2, following termination of CP translation. It is possible that previously proposed unidentified host factors (Soldevila & Ghabrial, 2000) might play a role in the reformation and stabilization of the secondary structure following CP translation.

Phylogenetic analyses of HvV190S and other members of the genus *Victorivirus* reveal that they are more closely related to each other than to any members of other genera in the family *Totiviridae*. Interestingly,

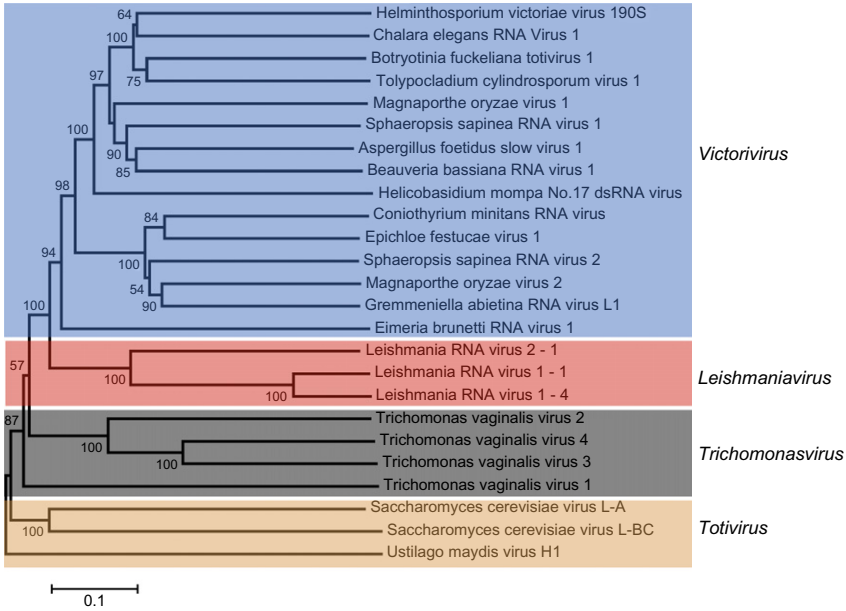

Figure 11.3 Neighbor-joining phylogenetic tree for the family *Totiviridae*. The tree was constructed from complete aa sequences of RdRps of representative members and probable members of the family. The aa sequences were aligned using the program CLUSTAL X2, and the tree was generated for codon positions using the MEGA5 phylogenetic package. Bootstrap percentages out of 2000 replicates are indicated at the nodes. Blue, red, gray, and brown shading, respectively, highlight the assignments of individual viruses to the genera *Victorivirus, Leishmaniavirus*, *Trichomonasvirus*, and *Totivirus*.

victoriviruses are more closely related to protozoan totiviruses than to the totiviruses that infect yeast and smut fungi (Fig. 11.3). Although HvV190S was originally classified in the genus *Totivirus*, it is obvious that it is phylogenetically distantly related to members of this genus. Thus, removal of HvV190S from *Totivirus* and establishment of the new genus *Victorivirus* to accommodate HvV190S and HvV190S-like viruses that infect filamentous fungi are highly justified (Ghabrial & Nibert, 2009).

3.2. Helminthosporium victoriae virus 145S (HvV145S)—family *Chrysoviridae*

Prior to availability of sequence information, HvV145S and Penicillium chrysogenum virus (PcV) were placed under the genus *Chrysovirus*, family *Partitiviridae* (with PcV designated as the prototype strain of the genus).

The belief was that these viruses (with three or four detectable segments) have bisegmented genomes coding for RdRp and CP and any additional segments were thought to represent satellite or defective RNA molecules. This confusion was clarified when the genomes of HvV145S (Ghabrial, Havens, & Annamalai, 2013; Ghabrial, Soldevila, & Havens, 2002) and PcV (Jiang & Ghabrial, 2004) were completely sequenced and shown to be quadripartite; this eventually led to the creation of the family *Chrysoviridae* (Jiang & Ghabrial, 2004). The genome of HvV145 comprises four dsRNA segments (2.7, 2.9, 3.1, and 3.6 kbp in length); each is monocistronic and has a unique sequence (Ghabrial et al., 2002, 2013). Like the prototype PcV, the HvV145S dsRNAs share common, highly conserved domains at their 5′ (Fig. 11.4A) and 3′ termini (Ghabrial, 2008a; Ghabrial et al., 2002, 2013). Northern hybridization analysis using cloned cDNA probes representing the four dsRNA segments showed that each segment has a unique sequence; no sequence homology to corresponding PcV segments or to the genomic dsRNA of the coinfecting HvV190S was detected (Fig. 11.4B). The 5′ UTRs of HvV145S segments are relatively long, between 200 and 400 nts in length, and their sequences have the potential to form extensive secondary structures. Direct comparison of the nucleotide sequences have revealed that, in addition to the strictly conserved 5′ and 3′ termini, there are regions of high sequence similarity within the 5′ UTRs and 3′ UTRs among all four dsRNAs. A highly conserved 75-nt region with almost 90% identity is present at the 5′ UTR of all four dsRNAs (designated "box 1"). A second region of strong sequence similarity is positioned immediately downstream of the highly conserved box 1. This region consists of a stretch of 30–35 nt (with sequence similarity above 80%) and is composed of a reiteration of the sequence "CAA," which depicts a strong resemblance to the $(CAA)_n$ repeats present in the 5′-UTRs of tobamoviruses (Gallie & Walbot, 1992). The poly (CAA) region of tobamoviruses has been reported to function as translational enhancers (Gallie & Walbot, 1992). Whether the HvV145S "CAA" repeats function like the translational regulatory elements of tobamoviruses has yet to be determined.

HvV145S dsRNA1 encodes the RdRp, dsRNA2 codes for the CP, and dsRNAs 3 and 4 code for proteins of unknown function. Assignment of numbers 1–4 to PcV dsRNAs was made according to their decreasing size. Following the same criterion used for PcV, the dsRNAs associated with HvV145S and other chrysoviruses were accordingly assigned the numbers 1–4. Sequence comparisons, however, indicated that dsRNA3s of Hv145SV, Amasya cherry disease-associated chrysovirus (ACDACV), and

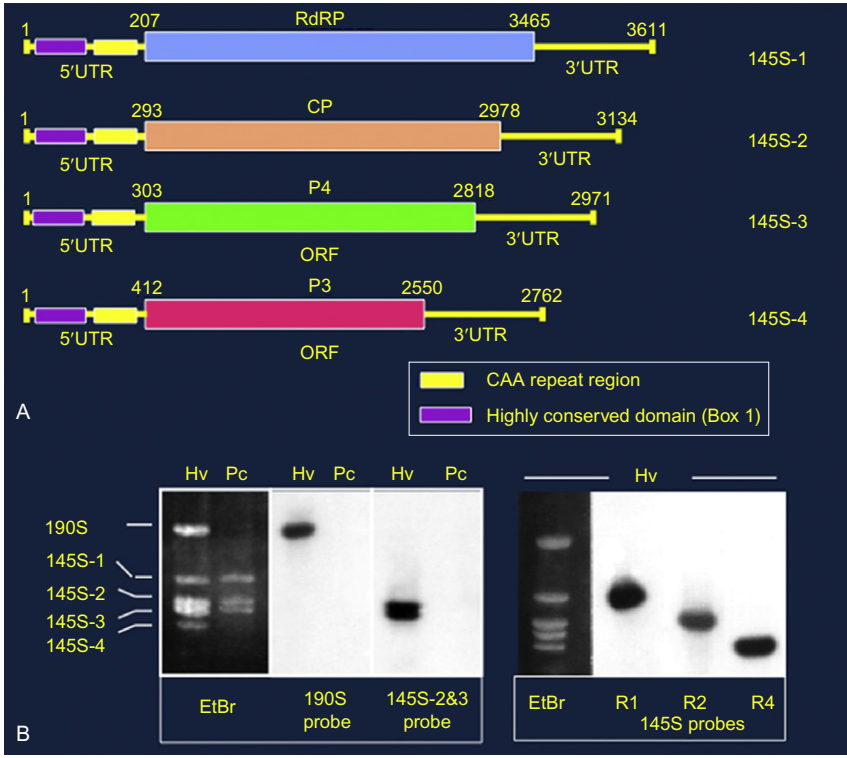

Figure 11.4 (A) Genome organization of Helminthosporium victoriae virus145S (HvV145S). The genome consists of four dsRNA segments, each of which is monocistronic. The RdRp ORF (nt positions 207–3465 on dsRNA1), the CP ORF (nt positions 293–2978 on dsRNA2), the p3 ORF (nt positions 412–2250 on dsRNA4), and the p4 ORF (nt positions 303–2818 on dsRNA3) are represented by rectangular boxes. Note that, unlike PcV, the prototype member of *Chrysovirus*, HvV145S dsRNA 3 codes for P4 and dsRNA 4 codes for P3 (see text). The purple-shaded box near the 5′ end represents a highly conserved domain (box 1), the yellow-shaded box downstream of the purple box is composed of a reiteration of the sequence "CAA." (B) Northern hybridization analysis using cloned cDNA probes representing the four HvV145S dsRNA segments and the HvV190S dsRNA. Results showed that each of the HvV145S dsRNAs has a unique sequence and that they lack sequence homology to both the chrysovirus PcV (lane Pc) and the coinfecting HvV190S. Lanes labeled "Hv" contains all four HvV145S dsRNA segments plus HvV190S dsRNA.

possibly Fusarium oxysporum chrysovirus 1 (FoCV1; based on partial sequence) are in fact the counterparts of PcV dsRNA4 rather than dsRNA3. Likewise, dsRNA4 of these chrysoviruses are the counterparts of PcV dsRNA3. Since PcV was the first chrysovirus to be characterized at the molecular level and to avoid confusion, the protein designations P3 and P4 as used for PcV

were adopted and referred to as chryso-P3 and chryso-P4 (Ghabrial, 2008a). Thus, whereas the chryso-P3 protein represents the gene product of PcV dsRNA3, it comprises the corresponding gene product of Hv145SVdsRNA4, and so on.

Whereas the prototype PcV dsRNA3 codes for its chryso-P3 protein, Hv145SV, ACDACV, and FoCV1 dsRNA4s encode the corresponding chryso-P3s. Although the functions of chryso-P3 and P4 are not known, sequence analysis and database searches offer some clues. ProDom database searches reveal that chryso-P3 sequences share a "phytoreo S7 domain" with a family (pfam07236:Phytoreo_S7; NBCI) consisting of several phytoreovirus P7 proteins known to be viral core proteins with nucleic acid binding activities. The consensus protein sequence for the three chrysoviruses is [X(V/I)V(M/L) P(A/M)G(C/H) GK(T/S)T-(L/I)]. Phytoreovirus P7 proteins bind to their corresponding P1 (transcriptase/replicase) proteins, which bind to the genomic dsRNAs. It is of interest, in this regard, that the N-terminal regions of all chryso-P3s (encompassing the amino acids within positions 1–500) share significant sequence similarity with comparable N-terminal regions of the putative RdRps encoded by chrysovirus dsRNA1s. The regions in the dsRNA1-encoded proteins with high similarity to chryso-P3 occur upstream of the eight highly conserved motifs characteristic of RdRps of dsRNA viruses of simple eukaryotes. The significance of this sequence similarity to the function of chryso-P3 is not known for certain, but one may speculate that the N-terminal region of these proteins may play a role in viral RNA binding and packaging. The chryso-P4 encoded by chrysoviruses contains the motif PGDGXCXXHX. This motif (I), along with motifs II (with a conserved K), III, and IV (with a conserved H), form the conserved core of the ovarian tumor, gene-like superfamily of predicted cysteine proteases (Covelli et al., 2004). Multiple alignments showed that motifs I–IV are also present in other viruses including Agaricus bisporus Virus 1, a tentative member of the family *Chrysoviridae*. Whether the dsRNAs of these viruses indeed code for the predicted proteases remains to be investigated.

The four HvV145S genome segments are encapsidated separately in identical capsids that are 350–400 Å in diameter (Ghabrial et al., 2002, 2013). BLAST searches of the HvV145S RdRp amino acid sequence showed that it shared significant sequence identity with ACDACV RdRp (42%) followed by the RdRps of Fusarium oxysporum chrysovirus 1 (FoCV1), Cryphonectria nitscheki chrysovirus 1 (CnCV1), PcV, Verticillium dahliae chrysovirus 1 (VdCV1), and Aspergillus fumigatus chrysovirus (AfCV) (41%, 40%, 39%, 39%, and 39%, respectively). High

similarities were also found with the RdRps of several members of the family *Totiviridae* (Jiang & Ghabrial, 2004). Interestingly, no significant hits were detected with any of the viruses in the family *Partitiviridae,* another validation for the removal of chrysoviruses from the family *Partitiviridae* and their placement in the recently created family *Chrysoviridae* (Jiang & Ghabrial, 2004). A neighbor-joining phylogenetic tree constructed based on full-length amino acid sequences of RdRps of members and probable members of the family *Chrysoviridae*, as well as selected members of the family *Totiviridae* (Fig. 11.5) is consistent with the sequence identity inferences made earlier. Interestingly, the phylogenetic tree also defines two clusters of chrysoviruses, those in which segment 3 codes for chrysoP3 (PcV, AfCV, CnCV1 and VdCV1, upper cluster) and those in which segment 3 codes for chrysoP4 (HvV145S, ACDACV and FoCV1, lower cluster).

PcV dsRNAs 3 and 4 differ in length by only 74 bp (Jiang & Ghabrial, 2004); therefore, they comigrate when separated by agarose gel electrophoresis.

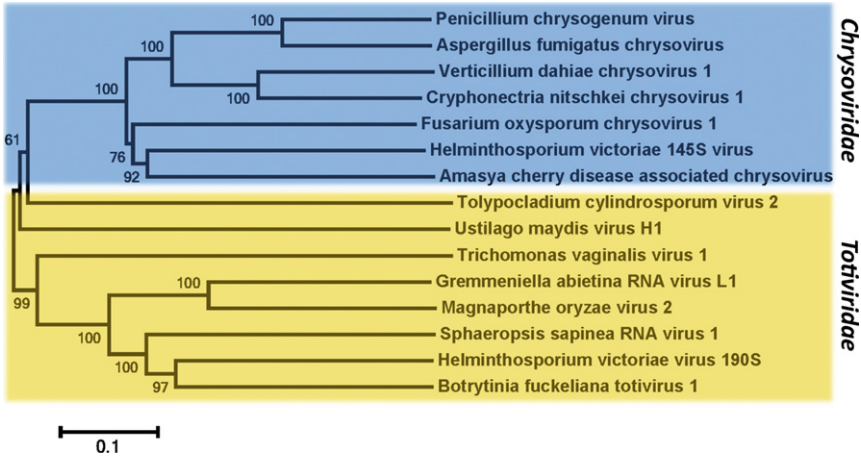

Figure 11.5 Neighbor-joining phylogenetic tree for the family *Chrysoviridae* and selected members of *Totiviridae*. The tree was constructed from complete aa sequences of RdRps of representative members and probable members of the family. The aa sequences were aligned using the program CLUSTAL X2, and the tree was generated for codon positions using the MEGA5 phylogenetic package. Bootstrap percentages out of 2000 replicates are indicated at the nodes. Note that high similarities (BLAST hits of 5e–13 or lower) were found between the HvV145S RdRp and the RdRps of several members of *Totiviridae*, mostly members of the genera *Victorivirus* and *Trichomonasvirus*. Interestingly, no significant hits were evident with any of the viruses in the family *Partitiviridae*, another validation for the removal of chrysoviruses from the family *Partitiviridae* and their placement in the family *Chrysoviridae*.

Sequencing analysis and *in vitro* coupled transcription–translation assays showed that each of the four PcV dsRNAs is monocistronic, as each dsRNA contains a single open reading frame and each is translated into a single major product of the size predicted from its deduced amino acid sequence. Thus, the fact that PcV virions contain four distinct dsRNA segments has clearly been established (Jiang & Ghabrial, 2004). Unlike PcV, dsRNAs 3 and 4 from other chrysoviruses including HvV145S are clearly resolved from each other when purified dsRNA preparations are subjected to agarose gel electrophoresis (e.g., see Fig. 11.4B, lanes Hv).

3.3. Viral etiology of the *H. victoriae* disease

In addition to transmitting the disease phenotype and associated viruses by hyphal anastomosis, the disease is also transmitted by incubating fusing protoplasts from virus-free fungal isolates with purified virions containing both HvV190S and HvV145S (Ghabrial & Mernaugh, 1983). The frequency of infection and stability of the newly diseased colonies, however, were very low. We have recently been successful in transfecting *H. victoriae* protoplasts with purified HvV190S particles using the transfection conditions of Sasaki, Kanematsu, Onoue, Oyama, and Yoshida (2006). The transfected colonies exhibited disease symptoms, and virus infection was verified by dsRNA analysis and RT-PCR (unpublished data). Furthermore, purified HvV190S virions were demonstrated to transfect mutant *Cryphonectria parasitica* (Δ*dcl-2*) and confer hypovirulence on infected colonies (Xie, Lin, Suzuki & Ghabrial, unpublished data). Curiously, disruptants Δ*dcl-2* become much more susceptible to hypoviruses and mycoreoviruses compared with the wild-type strain (Ghabrial & Suzuki, 2009). As an alternative approach to provide evidence for viral etiology, a hygromycin B resistance-based transformation system for *H. victoriae* (Li et al., 2011, 2013) was earlier developed and used to transform *H. victoriae* virus-free isolates with full-length cDNA clones of HvV190S or HvV145S dsRNAs. The HvV190S cDNA was inserted downstream of the *Cochliobolus heterostrophus GPD1* promoter and upstream of the *Aspergillus nidulans trpC* terminator signal. The hygromycin-resistant transformants expressed HvV190S CP, as determined by Western blot analysis. Transformation of a normal virus-free fungal isolate with a full-length cDNA of HvV190S dsRNA, but not with cDNAs corresponding to the four HvV145S dsRNAs conferred a disease phenotype in some transformants (Ghabrial, 2008b). Symptom severity varied among the transformants from symptomless to severely stunted and highly sectored (Ghabrial, 2008b, Li et al., 2013). Symptom severity correlated well with

the level of viral capsid accumulation in the transformants (Li et al., 2013). Empty capsids accumulated to significantly higher levels in transformants exhibiting the disease phenotype. Although the RdRp was expressed and packaged, no dsRNA was detected inside the virus-like particles or in the total RNA isolated from mycelium. Despite the inability to launch dsRNA replication from the integrated viral cDNA (this is also true with the ScV-L-A virus), the demonstration that ectopic HvV190S cDNA is transcribed and translated and that the resultant transformants exhibit a disease phenotype (Ghabrial, 2008b, Li et al., 2013) provides further convincing evidence for a viral etiology for the disease of *H. victoriae*. Taken together, the results of the transformation/transfection experiments suggest that HvV190S is the primary cause of the disease of *H. victoriae* and that HvV145S has apparently no role in disease development. Like other chrysoviruses, HvV145S has no effect on colony morphology of infected fungal isolates.

4. HOST GENES UPREGULATED BY VIRUS INFECTION

4.1. Hv-p68

H. victoriae p68 protein (Hv-p68) is a multifunctional protein with alcohol oxidase/protein kinase/and RNA-binding activities. It copurifies with viral dsRNAs, mostly those of HvV145S, in a top component that is resolved as a discrete band near the meniscus when purified virion preparations from diseased *H. victoriae* isolates are subjected to sucrose density gradient centrifugation (Soldevila et al.,2000). SDS-PAGE analysis of the top component reveals a single major protein with an estimated molecular mass of 68 kDa (Hv-p68). The discovery of the Hv-p68 enriched top component was a pleasant surprise as it allowed its purification and characterization (Soldevila et al., 2000).

The gene encoding Hv-p68 has been isolated from a cDNA library generated in lambda phage using mRNA from a virus-infected fungal isolate. The complete nucleotide and deduced amino acid sequences of Hv-p68 have been determined (Soldevila & Ghabrial, 2001). Sequence analysis revealed that Hv-p68 belongs to the large family of flavin-adenine dinucleotide (FAD)-dependent glucose-methanol-choline (GMC) oxidoreductases with 67–70% sequence identity to the alcohol oxidases of methylotrophic yeasts (Soldevila & Ghabrial, 2001). A molecular mass estimate of 550 kDa has been obtained for the native size of Hv-p68 using gradient-purified Hv-p68 and high-performance size-exclusion chromatography (Soldevila et al., 2000). Based on a molecular-mass of 68 kDa, as determined by SDS-PAGE, the

native-size estimate of 550 kDa suggested that Hv-p68 is an octomer. The oligomeric arrangement of Hv-p68 has been confirmed by electron microscopic examination (Soldevila et al., 2000), which revealed the presence of octad aggregates of approximately 150–200 Å in diameter comprised of two tetragons aligned face to face. The combined results of SDS-PAGE, size exclusion chromatography, and electron microscopy strongly suggest that Hv-p68, like some other oxidases, is present *in vivo* as an oligomeric protein consisting of eight identical subunits (Soldevila et al., 2000).

Expression of the Hv-p68 gene at the transcriptional level has been examined (Soldevila & Ghabrial, 2001). Elevated levels (10- to 20-fold) of the Hv-p68 transcript were found in the virus-infected fungal isolates compared to the virus-free ones. This finding is in agreement with the higher levels of protein detected by Western blot analysis in a virus-infected isolate (Soldevila et al., 2000; Soldevila & Ghabrial, 2001). Unlike the alcohol oxidases from methylotrophic yeasts, the Hv-p68 purified from fungal extract shows low levels of methanol oxidizing activity. Furthermore, the levels of Hv-p68 transcripts are not significantly different in methanol-supplemented versus glucose-supplemented cultures (Soldevila & Ghabrial, 2001), indicating that Hv-p68 transcription is neither inducible by methanol nor repressed by glucose. Altogether, these data suggest that the Hv-p68 promoter may not be regulated in the same fashion as the promoters for the alcohol oxidases of yeast and that the Hv-p68 promoter is upregulated during the course of viral infection of *H. victoriae*.

The natural substrate for Hv-p68 is not known, but the structurally similar alcohol oxidases are known to oxidize primary alcohols irreversibly to toxic aldehydes. Overexpression of Hv-p68 and subsequent putative accumulation of toxic intermediates have been hypothesized as a possible mechanism underlying the disease phenotype of virus-infected *H. victoriae* isolates. Overexpression of Hv-p68 in virus-free fungal isolates, however, resulted in a significant increase in colony growth and did not induce a disease phenotype (Zhao, Havens, & Ghabrial, 2006). The finding that colonies overproducing the Hv-p68 protein did not exhibit the disease phenotype and grew more rapidly than the nontransformed wild type suggests that accumulation of toxic aldehydes did not occur and that such aldehydes were probably assimilated into carbohydrates via the xylulose monophosphate pathway (Reid & Fewson, 1994).

Hv-p68, which copurifies with viral dsRNAs as a top component in sucrose gradient centrifugation of virus preparations, has been examined for RNA-binding activity by gel retardation and Northwestern analysis

(Soldevila et al., 2000; Soldevila and Ghabrial, 2001). When ^{32}P end-labeled 190S and 145S dsRNAs were incubated with increasing amounts of Hv-p68 followed by agarose gel electrophoresis, a band of free dsRNA and a band of retarded dsRNA (RNA-protein complex) were detected at the lower protein concentrations. However, at higher protein concentrations, only the band of retarded dsRNA was observed. HvV190S and HvV145S dsRNA and yeast tRNA in molar excess amounts were tested as competitors in binding reactions. A 5- to 10-fold molar excess of the unlabeled 190S/145S dsRNAs, when added to the standard binding reaction, completely abolished binding to the probe. Yeast tRNA at 250-fold molar excess only partially competed with binding to the dsRNA probe (Soldevila et al., 2000). On the basis of Northwestern analysis and deletion mutants of bacterially expressed Hv-p68, the RNA-binding domain of Hv-p68 was mapped to the N-terminal region that contains a canonical ADP-binding β−α−β fold motif. Southern analysis of genomic DNA from several species of the genus *Cochliobolus* (anamorph, *Helminthosporium*) indicated that a single copy of the *Hv-p68* gene is present in all species of the genus *Cochliobolus* examined. The *Hv-p68* gene, however, was detected neither in *Penicillium chrysogenum* nor in two nonmethylotrophic yeasts, *S. cerevisiae* and *S. pombe* (Soldevila & Ghabrial, 2001).

Recent evidence (Ghabrial & Havens, 2013) strongly suggests that Hv-p68 is the cellular protein kinase responsible for phosphorylating the p88 HvV190S CP. From phosphoamino acid analysis, we determined that Hv-p68 is a serine/threonine protein kinase that catalyzes autophosphorylation and phosphorylation of casein and HvV190S CP. The cofactor flavin adenine dinucleotide (FAD), which is required for Hv-p68 activities, was demonstrated to be a strong competitive inhibitor of Hv-p68 kinase activity (Ghabrial & Havens, 2013).

4.2. *Victoriocin gene (vin)*

Victoriocin is a novel broad-spectrum, secreted, antifungal protein that is overproduced in virus-infected *H. victoriae* isolates (de Sá, Havens & Ghabrial, 2010). Culture filtrates of virus-infected *H. victoriae* isolates exhibit antifungal activity against a broad range of fungal and oomycete plant pathogens, including F*usarium solani*, *Phomopsis longicola*, *C. parasitica*, *Phytophthora parasitica* var. *nicotianae*, *Peronospora tabacina*, and the opportunistic human pathogens *Aspergillus fumigatus* and *Candida albicans*. de Sá, Havens, et al. (2010) purified victoriocin from culture filtrates using a multistep procedure that includes ultrafiltration and reverse-phase high-performance liquid chromatography (RP-HPLC). A well assay similar to that shown in Fig. 11.6A is used to test culture filtrates or RP-HPLC fractions for

antifungal activity. SDS/PAGE and Western blot analysis of active RP-HPLC fractions, as determined by the well assay (Fig. 11.6B), reveals the presence of two major proteins, P10 (the mature form of victoriocin) and P30 (a cell wall protein; see Section 4.3).

The fact that the yeast and smut strains of fungi that secrete killer proteins (killer toxins) are infected with totiviruses similar to HvV190S stimulated the search for viral origin for the antifungal activity associated with culture

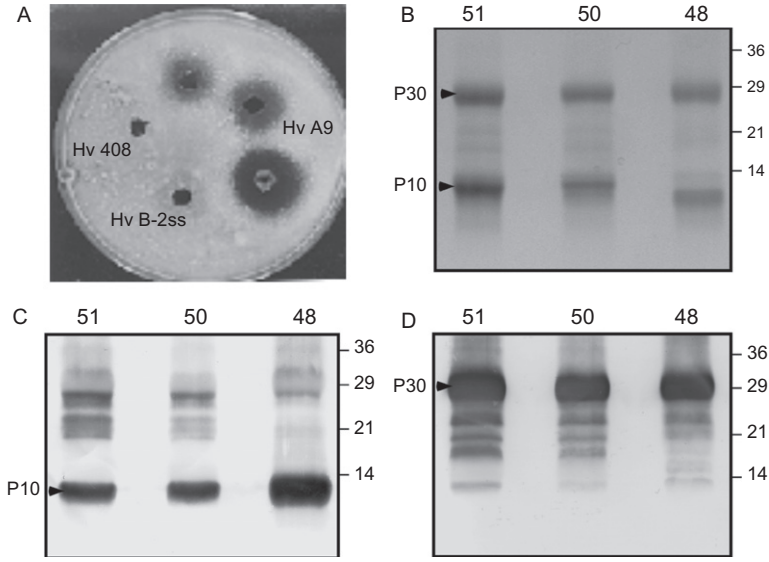

Figure 11.6 (A) Antifungal activity of *Helminthosporium victoriae* culture filtrates using the "well assay." Plates of potato dextrose agar, prepared in 0.05 M citrate buffer, pH 4.5, were seeded with spore suspensions of *Penicillium chrysogenum*, and wells were cut with a cork borer and filled with the assay solutions. (A) Antifungal activity of twofold serial dilutions of culture filtrates of the virus-infected strain A-9 is demonstrated in wells 1–3. No antifungal activity was detected with culture filtrates of virus-free strains 408 and B-2ss (wells 4 and 5, respectively). (B) Sodium dodecyl sulfate polyacrylamide gel electrophoresis of reverse-phase high-performance liquid chromatography retention fractions collected at 48, 50, and 51 min. The gel was stained with Coomassie blue and the positions of P10 and P30 proteins are indicated to the left. (C, D), Western blot analysis of two major proteins, P10 (the mature victoriocin protein) and P30 (a cell wall protein) purified from culture filtrates of the virus-infected *Helminthosporium victoriae* strain A-9. Proteins were transferred from replicate gels to polyvinylidene difluoride membranes, and the membranes were probed with the antiserum to P10 (panel C) or P30 (panel D). Note that the antiserum prepared against P10 reacted strongly with its homologous P10 protein and with larger, possibly related precursor proteins (see text), but not with P30. *Adapted from P. B. de Sá, W. M. Havens and S. A. Ghabrial, 2010, Characterization of a novel broad-spectrum antifungal protein from virus-infected* Helminthosporium (Cochliobolus) victoriae. Phytopathology, *100, 880–889.*

filtrates of *H. victoriae*. The killer proteins from virus-infected yeast and smut strains are encoded by satellite dsRNAs that are dependent on helper totivirus for replication and encapsidation (Schmitt & Breinig, 2006; Wickner, 1996). No satellite dsRNAs, however, were detected in association with HvV190S infection (Ghabrial & Nibert, 2009). Nevertheless, victoriocin, which is encoded by a host chromosomal gene designated *victoriocin* (or *vin*), is structurally similar to killer proteins. The mature victoriocin (P10) is expressed *in vivo* as a 183-amino-acid preprotoxin precursor. This ~20-kDa preprovictoriocin has a predicted, secretory pathway signal peptide, and cleavage between Ala^{23} and Val^{24} releases a predicted proprotein of 17 kDa into the secretory pathway. Further cleavage of the proprotein by a subtilisin/kexin-like proprotein convertase in the latter part of the Golgi complex is predicted to release the mature victoriocin of 86 amino acids with a molecular mass of ~10 kDa (Fig. 11.7). The protease Kex2 (kexin) of *S. cerevisiae* is the prototype of a family of serine proteases that process precursor proteins to active proteins in eukaryotes. It is a Ca^{2+}-dependent transmembrane protease present in a trans-compartment of the yeast Golgi that contains late-processing enzymes (Bryant & Boyd, 1993). Kex2 is necessary for the production and secretion of the mature alpha factor and killer toxins in *S. cerevisiae* at paired basic sites, optimally at Lys-Arg or Arg-Arg (Rockwell & Fuller, 1998). Kexin-like proteins are ubiquitously found in eukaryotes and their occurrence in *H. victoriae* is expected. The mature victoriocin and the predicted precursors (pro- and preprotoxin) were clearly detected in the virus-free *H. victoriae* isolates that were overexpressing the *vin* gene (de Sá, Li, Havens, Farman, & Ghabrial, 2010).

The similarities between victoriocin and the killer protein zygocin, a monomeric protein toxin secreted by a totivirus-infected killer strain of the osmotolerant spoilage yeast *Zygosaccharomyces bailii* (Weiler & Schmitt, 2005), are of considerable interest. Whereas the killer proteins of *S. cerevisiae* (K1, K2, and K28) and *Ustilago maydis* (KP1, KP4, and KP6) are active only against yeasts and smuts, respectively (Bruenn, 2004; Wickner, 1996), zygocin, like victoriocin, has a broad-spectrum antifungal activity against human and phytopathogenic yeasts and filamentous fungi (de Sá, Havens, et al., 2010). On the other hand, zygocin, like other killer proteins, is encoded by a satellite dsRNA that is dependent on a totivirus, Zygosaccharomyces bailii virus, for replication and encapsidation (Schmitt & Breinig, 2006). Although there is a limited primary structure similarity (11% identity) between the two toxins, it is intriguing that the virally encoded zygocin and the chromosome-encoded victoriocin are so similar

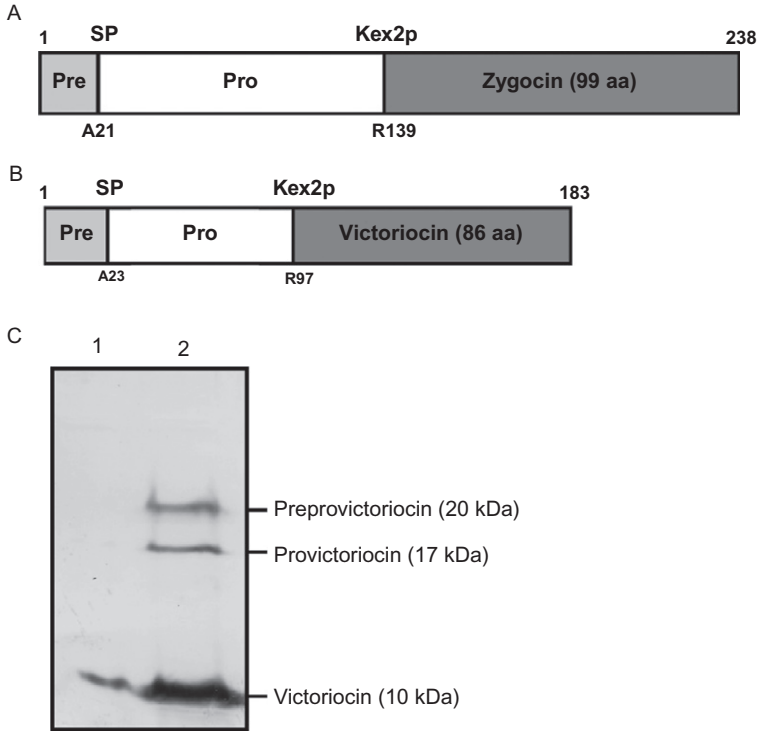

Figure 11.7 Schematic representations of preprovictoriocin (A) and preprozygocin (B). Processing sites are indicated by vertical lines with the name of the pertinent protease indicated above the diagram and the amino acid residue where cleavage occurs indicated below the diagram; signal peptidase (SP) and kexin-like protease (Kex2p). (C) Western blot analysis of proteins extracted from a virus-free *Helminthosporium victoriae* isolate transformed with the victoriocin (*vin*) construct pCB-*vin* (lane 2; pCB-*vin* contains full-length *vin* coding region and flanking 5′ and 3′ untranslated regions) or empty vector (lane 1; pCB1004) (de Sá, Havens,et al., 2010; de Sá, Li, et al., 2010). ppV, preprovictoriocin; pV, provictoriocin; and V, mature victoriocin. Note that *vin* is an endogenous host gene and its translation product can be detected at low levels (lane 1).

in their overall structure (Fig. 11.7) and hydrophobicity profiles (de Sá, Havens, et al., 2010). Each preprotoxin consists of a hydrophobic N-terminal secretion signal, followed by a potentially N-glycosylated pro-region and terminating in a classical Kex2p endopeptidase cleavage site that generates the N-terminus of the mature and biologically active protein toxin in a late Golgi compartment (Fig. 11.7; de Sá, Havens, et al., 2010; Schmitt & Breinig, 2006; Weiler & Schmitt, 2005). The conspicuous similarity of these two proteins (both secreted and both processed by signal peptidase and kexin-like protease) suggests that the zygocin toxin might

have been captured by the virus from a cellular transcript because the victoriocin protein is encoded by a nuclear gene.

It is worth noting that victoriocin has a short scorpion toxin family signature motif at its carboxyl terminal region (Bontems, Roumestand, Gilquin, Ménez, & Toma, 1991). Furthermore, it exhibits the conserved CSαβ- and γ-core motifs common to members of the scorpion toxin-like family (de Sá, Havens, et al., 2010). Scorpion toxins are part of one of the functionally most diverse structural superfamilies in single-domain proteins, most of whose functions are associated with host defense mechanisms. Membrane channels are a major target for the various toxins produced by scorpions and other venomous animals (Dauplais et al., 1997). Furthermore, victoriocin shares structural and functional motifs with defensins, which represent a diverse set of antimicrobial peptides known to be part of the innate immune systems of eukaryotes. Defensins are active against fungi, bacteria, and viruses. These small proteins are characterized by having an N-terminal signal sequence, by being highly divergent, mature proteins with the exception of conserved cysteine residues, and by including defensin motifs. Victoriocin is also characterized by an N-terminal signal peptide and shares the conserved CSαβ- and γ-core consensus motifs, characteristics of defensins (de Sá, Havens, et al., 2010; Yount and steadman, 2004). Because defensin expression can be induced by pathogen inoculation and environmental stress, victoriocin may be viewed as a fungal defensin that is induced by virus infection. Insect and mammalian defensins, but not plant defensins, are known to form voltage-regulated multimeric channels in the membranes of susceptible cells (de Sá, Havens, et al., 2010). The mode of action of victoriocin, like many antifungal proteins, is not known. However, considering its similarities to some killer proteins (e.g., zygocin), defensins, and neurotoxins, it is expected to target cytoplasmic membrane functions by forming cation-selective ion channels.

In BLAST searches, the only known protein with significant amino acid sequence identity to the 20-kDa protein (preprovictoriocin) was the IDI-2 precursor of *Podospora anserina* (accession no. AF500213) showing 31% identity along a stretch of 161 amino acids. The IDI-2 protein, like victoriocin, is a small, cysteine-rich protein with a signal peptide. Interestingly, expression of three *idi* genes including *idi-2* in *P. anserina* was shown to correlate with the cell death reaction associated with nonallelic vegetative incompatibility (Bourges, Groppi, Barreau, Clave, & Begueret, 1998).

We have recently constructed an *H. victoriae* genomic DNA library in a cosmid vector and a cosmid clone carrying the *vin* gene and flanking

sequences was isolated and used to generate constructs for transformation of virus-free and virus-infected *H. victoriae* isolates with the *vin* gene. Culture filtrates of the virus-free *vin* transformants exhibited high levels of antifungal activity compared with that detected for the nontransformed virus-free wild-type strain, which exhibited little or no antifungal activity. Moreover, transformation of a wild-type virus-infected *H. victoriae* strain with the *vin* gene resulted in still higher production of victoriocin and higher antifungal activity in the culture filtrates of the *vin* transformants compared with the virus-infected wild-type strain. Taken together, these results indicate that victoriocin is the primary protein responsible for the antifungal activity in culture filtrates of virus-infected *H. victoriae* isolates and that virus infection upregulates the expression of victoriocin. Overproduction of victoriocin may give the slower-growing virus infected fungal strains some competitive advantage by inhibiting the growth of other fungi (de Sá, Li, et al., 2010).

4.3. *P30* gene

In addition to the broad-spectrum, antifungal protein, victoriocin, a cell wall protein, designated P30, was also overproduced in the culture filtrates of virus-infected *H. victoriae* isolates (Fig. 11.6B). Full-length cDNA and genomic clones of *P30* coding region have been constructed and sequenced (de Sá, Havens, et al., 2010; Xie & Ghabrial, 2013). Sequence analysis of *P30* indicated that it lacks introns and that the P30 protein is a secreted protein with a predicted signal peptide that is cleaved between amino acid positions 18 and 19 (Ala/Lys). BLASTP search of the deduced amino acid sequence revealed similarity between P30 and PhiA cell wall proteins (Melin, Schnuürer, & Wagner, 2003) from several *Aspergillus* spp. including *Emericella* (*Aspergillus*) *nidulans* (37% identity), *A. fumigatus* (37% identity), *A. clavatus* (35% identity), and also to the alkaline foam protein A precursor protein (AfpA) of *Fusarium culmorum* (37% identity). Furthermore, P30 contains the sequence motifs SGMGQG and ACP present in the highly conserved core region of "fungispumins," a recently described class of proteins (Zapf et al., 2007). PhiA is involved in phialide development in *A. nidulans* and is overexpressed in response to treatment with bafilomycin with antifungal and antibacterial activities (Melin et al., 2003). The natural function of fungispumins remains to be elucidated. The role of P30, if any, in the antifungal activity exhibited by culture filtrates of virus-infected *H. victoriae* isolates is not clear.

The overexpression of P30 may represent an indirect response to the presence of the secreted antifungal protein victoriocin in a manner comparable to the overexpression of the homologous PhiA proteins by *Aspergillus*

spp. following treatment with the antifungal agent bafilomycin and the resultant inhibition of vacuolar ATPases (Melin et al., 2003). It was of interest to determine whether overexpression of P30, a homologue of PhiA, plays a role in the development of the disease phenotype (short, swollen hyphae) of virus-free *H. victoriae* isolates, considering the similarity in hyphal morphology between the disease phenotype in *H. victoriae* (Ghabrial et al., 1979) and *A. nidulans* that overexpresses PhiA following treatment with the antifungal agent concanamycin (Melin, Schnuürer, & Wagner, 2002). Colonies generated from virus-free protoplasts transformed with a *P30* overexpression vector were stunted with significantly smaller diameter than control colonies (Xie & Ghabrial, 2013). It is not known, however, whether the disease phenotype in *H. victoriae* is associated with inhibition of vacuolar ATPases.

5. HvV190S CAPSID STRUCTURE

HvV190S virions have isometric capsids that are relatively smooth and featureless with no obvious protrusions, as seen in transmission electron micrographs of unstained, vitrified specimens (Fig. 11.8A) (Dunn et al., 2013). A three-dimensional cryo-reconstruction of the HvV190S virion, computed from 20,904 images and estimated at a resolution of 7.1 Å, showed that the icosahedral capsid reaches a maximum diameter of 462 Å at the fivefold vertices and diameters of 356 and 368 Å at the threefold and twofold axes, respectively (Fig. 11.8B). The thickness of the capsid is ~35 Å on average but drops to a minimum of just 6 Å at the threefold axes. The inner surface of the capsid is also quite smooth, except for small, mushroom-shaped cavities that extend radially outward along the fivefold axes (Fig. 11.8C and D). The dsRNA genome, protected by the capsid, is arranged in five, roughly spherical, concentric shells whose average spacing (~30 Å) compares favorably with the genome spacings observed in ScV-L-A and other dsRNA fungal viruses (Naitow, Tang, Canady, Wickner, & Johnson, 2002; Ochoa et al., 2008, Pan et al., 2009; Tang et al., 2008). The outermost shell of dsRNA lies ~17 Å away from the inner wall of the capsid, except near the twofold axes, where some diffuse density may represent potential points of contact between genome and capsid. Cross-section (equatorial) views of the HvV190S virion demonstrate that the capsid contains numerous punctate and linear density features (Fig. 11.8D). These are ascribed to α-helical secondary-structure elements that lie perpendicular to or in the plane of the section, respectively. Spherical density sections of the

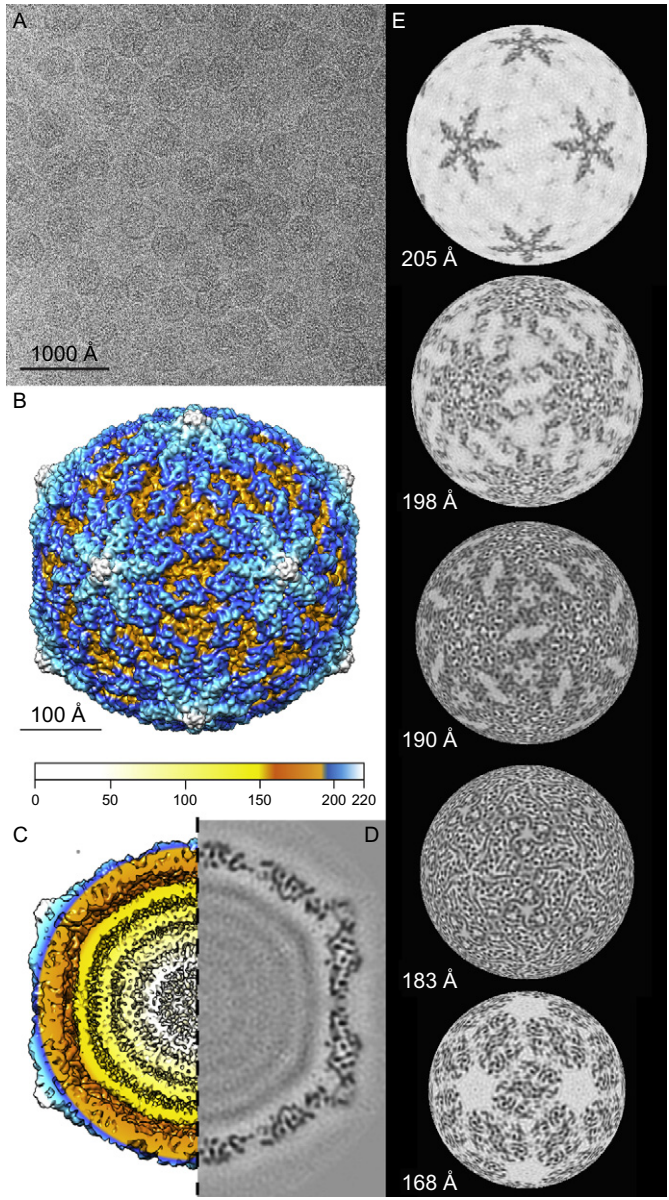

Figure 11.8 Structure of the HvV190S virion. (A) Electron micrograph of an unstained, vitrified sample of HvV190S virions. (B) Radial, color-coded, surface view along a twofold axis of the HvV190S virion cryoreconstruction. (C) Same as (B), with the front half of the density map removed to show the particle interior and only showing the left quadrant. (D) Planar, central density section (~1 Å thick) from the right half of the HvV190S virion cryo-reconstruction (high- and low-density features are depicted in black and white, respectively). (E) Spherical density projections (each ~1 Å thick) from the HvV190S virion cryo-reconstruction at select radii, as indicated in each panel, with highest and lowest density features depicted in black and white, respectively. Intersubunit interactions are most prevalent as well as dense at a radius of 183 Å.

HvV190S capsid structure confirm that these same features are distributed throughout the capsid at all radii (Fig. 11.8E).

Close inspection of the HvV190S capsid surface (Fig. 11.7B) reveals the presence of 120 morphological features that are consistent with a "$T=2$" icosahedral arrangement of subunits as found in the capsids or inner capsids of most other dsRNA viruses (Castón et al., 1997; Ochoa et al., 2008; Pan et al., 2009; Tang, Ochoa, et al., 2010). The high radii density features in the capsid adopt a staggered arrangement, with 60 copies of one "unit" clustered in groups of 5 about the 12 fivefold vertices and 60 copies of a similarly shaped second unit clustered in groups of 3 about the 20 threefold vertices. Both surface-exposed units have similar, globular head domains that project toward the fivefolds and similar, anchor-like tails that lie near the twofolds. Segmentation of the entire HvV190S capsid cryoreconstruction (Dunn et al., 2012) made it possible to assign all density features to either an "A" or a "B" subunit, labeled according to the distinct locations they occupy in the icosahedron (A nearest the fivefolds and B nearest the threefolds; Fig. 11.9A). Hence, the asymmetric unit of the icosahedron is an AB dimer (Fig. 11.9B), which consists of two chemically identical monomers (772 aa; calculated molecular mass of 81 kDa).

The segmentation process showed that both monomers have an overall morphology that, when viewed from outside the capsid, it has the shape of a complex quadrilateral (Fig. 11.9B). With the exception of the proximal and distal tips of the subunits, the segmented density maps for the A and B subunits superimpose quite closely, including nearly all of the recognizable secondary structural elements (Dunn et al., 2013). This strongly suggests that the tertiary structures of the subunits are nearly the same and they differ most in regions where intersubunit interactions are nonequivalent.

5.1. Comparison of the HvV190S capsid with that of other totiviruses

The capsid subunits of HvV190S and ScV-L-A share a striking resemblance in their overall morphologies. Given that ScV-L-A is the only totivirus whose high-resolution crystal structure has been determined to date (Naitow et al., 2002), an attempt was made to quantitatively fit as rigid bodies the A and B subunit structures into the segmented density maps of the corresponding HvV190S subunits (Dunn et al., 2013). As expected, because the ScV-L-A subunit is smaller than the HvV190S subunit (680 vs. 772 aa) and 29 residues at the C-termini were disordered and hence not resolved in the ScV-L-A X-ray crystal structure (Naitow et al., 2002), this fitting process

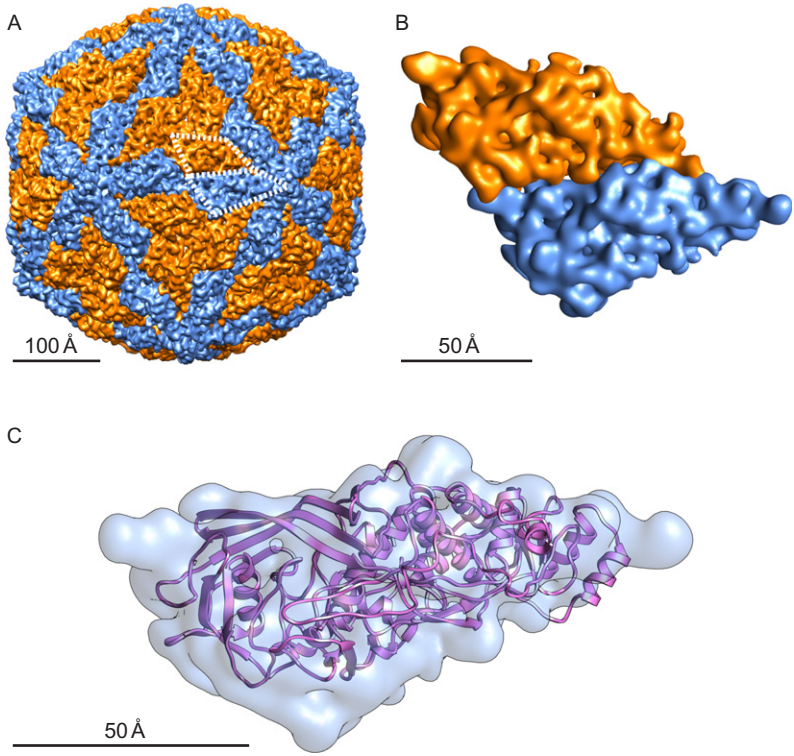

Figure 11.9 Subunit structure of HvV190S and comparison with ScV-L-A. (A) View along a twofold axis of a segmented version of the HvV190S cryoreconstruction with the A- and B-subunits colored in blue and orange, respectively. The A and B subunits in one asymmetric dimer are outlined with quadrilateral polygons. (B) Enlarged view of one asymmetric dimer in an orientation similar to that shown in panel (A). (C) View of the ScV-L-A A-subunit crystal structure (Naitow et al., 2002), represented as a purple ribbon model, fit as a rigid body into the segmented density map of the HvV190S A-subunit (blue transparent envelope), which is oriented like the A-subunit of panel (B).

left several regions of the HvV190S subunits unassigned. This included the proximal tip of the A-subunit and a portion of the proximal tip of B, the entire distal tips of both subunits, and a large portion of the long edge of each subunit. In addition, one side of the B-subunit density also remained unassigned. Of even more significance, with few exceptions, the tertiary folds of the HvV190S subunits differ substantially from those of the corresponding ScV-L-A subunits, as evidenced, for example, by misalignment of most of the prominent secondary structural features (Fig. 11.9C). Nonetheless, three separate segments of the ScV-L-A subunit structure did correlate quite

well with densities in the HvV190S map. These included in ScV-L-A two α-helices (helix 5: aa 120–139 and helix 13: aa 358–383) and an antiparallel β-sheet comprising three main (aa 26–38, 41–54, 587–600) and three small (aa 302–304, 487–491, 604–606) strands (Fig. 11.10). The helices form a central core region in each ScV-L-A subunit and correspond quite closely in size and location to tubular density features in each of the two HvV190S subunits. The β-sheet in each ScV-L-A subunit model nicely correlates with a large, plate-like density feature that occurs near the distal end and left side of each HvV190S subunit.

In the absence of a crystal structure for the HvV190S capsid or isolated capsid subunit, the secondary structure of the HvV190S subunit was assessed by means of prediction methods and, for validation, these same methods were used to assess the ScV-L-A subunit (Dunn et al., 2013). This validation led to a prediction for ScV-L-A that completely matched all the secondary structure

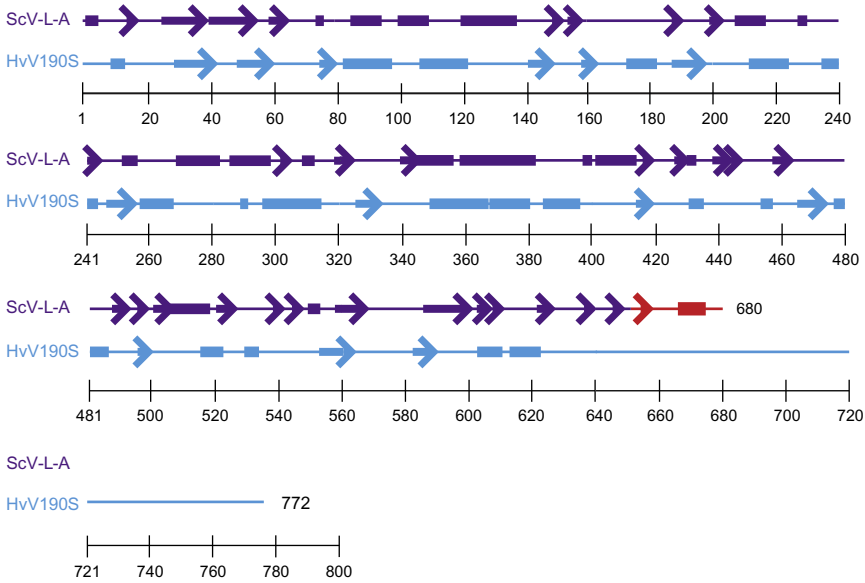

Figure 11.10 Comparison of the secondary structure of the ScV-L-A capsid protein to the predicted secondary structure of the HvV190S capsid protein. For the ScV-L-A subunit, the secondary structure for the first 651 residues (purple) was derived from the crystal structure (PDB ID 1M1C), and the structure of the remaining 29 residues (red) was predicted using the PSIPRED server (Dunn et al., 2013). PSIPRED was used to predict the entire secondary structure of the HvV190S subunit (blue). Rectangles, arrows, and lines are used, respectively, to represent schematically α-helix, β-strand, and random coil segments in both virus capsid proteins.

elements observed in the crystal structure (24.4% helix, 20.4% sheet, and 55.2% coil). For HvV190S, the predicted elements included 21% helix, 12% sheet, and 67% random coil. The result of these prediction and three-dimensional fitting analyses confirmed the earlier suggestion that the folds of the subunits of ScV-L-A and HvV190S differ significantly (Castón et al., 2006).

The apparent conservation of a pair of helices in the cores of the ScV-L-A and HvV190S subunits raises the question of whether this core structure might be shared by other or perhaps all totiviruses. To address this, secondary structure predictions were made for the CPs of several other members of the family *Totiviridae* (Dunn et al., 2013). These included six additional members of the genus *Victorivirus* (BfTV1, CmRV, GaRV-L1, SsRV2, CeRV-1, and SsRV1), single representative members of *Leishmaniavirus, Trichomonasvirus,* and *Giardiavirus*, (LRV-1, TVV-1 and GLV), and two unclassified members (EbRV1 and IMNV). The results of this analysis demonstrated high conservation among all victoriviruses, of not just the central core helices but also nearly every secondary element including the β sheets. This is completely consistent with the high levels of sequence identity that each victorivirus shares with HvV190S, which ranges from a maximum of 62% for BfTV1 to a minimum of 37% for CmRV (Dunn et al., 2013). Given this high level of conservation, all victoriviruses are expected to have nearly identical, smooth-shaped, "$T=2$" capsids like HvV190S. Though a similar helix core appears to be present in the other totiviruses, like ScV-L-A, there is no compelling evidence from the secondary structure analysis to suggest that the subunits of totiviruses outside the genus *Victorivirus* adopt the HvV190S tertiary structure.

Results of phylogenetic analysis based on complete amino acid sequences of the CP (Ghabrial & Nibert, 2009) or the RdRp (Fig. 11.3; this chapter) further support the conclusion that all victoriviruses are phylogenetically closely related to each other as they form one major cluster in the phylogenetic tree. On the other hand, victoriviruses are distantly related to members of the genus *Totivirus* (ScV-L-A and UmV-H1) that infect yeast and smut fungi. Interestingly, victoriviruses are more closely related to protozoan totiviruses than to the yeast and smut totiviruses. In this regard, the report that a protozoan totivirus, Eimeria brunetti RNA virus 1 (EbRV1), shares the victorivirus strategy for RdRp expression as a separate protein, with the RdRp start codon overlapping the CP stop codon in the −1 frame at an AUGA tetranucleotide motif, is of considerable interest (Fraga et al., 2006). EbRV is identified in the phylogenetic trees as the virus next most closely related to victoriviruses. Therefore, results of phylogenetic analyses

are in line with those of secondary and tertiary structure assessments of victoriviruses and other totiviruses.

6. CONCLUDING REMARKS

- Diseased isolates of *H. victoriae* are doubly infected with the victorivirus HvV190S and the chrysovirus HvV145S. Mixed infection, however, is not required for development of the disease phenotype. DNA transformation and transfection assays with purified virions strongly suggest that HvV190S is the major cause of the disease of *H. victoriae* and that HvV145S, like other chrysoviruses, does not appear to affect colony morphology.
- HvV190S, the prototype of the genus *Victorivirus*, family *Totiviridae*, is the best-characterized victorivirus. It utilizes a novel coupled termination–reinitiation strategy for expression of its RdRp from the downstream ORF. With elucidation of the RNA sequence determinants of the stop–restart strategy of HvV190S, it became apparent that the other 13 victoriviruses, even though less well characterized than HvV190S, utilize similar strategy for expressing their RdRps.
- With the availability of transformation/transfection systems for *H. victoriae*, the questions of whether virus infection affects victorin production and thus virulence could now be directly addressed.
- The multifunctional activities (alcohol oxidase, RNA binding, and protein kinase) of the cellular Hv-p68 have been demonstrated. Whereas the alcohol oxidase activity of Hv-p68 does not appear to play a role in disease development, the RNA binding and kinase activities are thought to be important for virus replication and RNA packaging.
- Victoriocin, the preprotoxin that is overexpressed in virus-infected *H. victoriae*, should be exploited for expression in economically important plants to provide broad protection against fungal and oomycete plant pathogens. Genomic as well as full-length cDNA clones of victoriocin are available for constructing plant expression vectors. It might be necessary, however, to replace the fungal signal peptide in victoriocin with a plant signal peptide for efficient secretion.
- The HvV190S virion structure was determined by electron cryomicroscopy and three-dimensional image reconstruction methods at 7.1-Å resolution. The capsid was found to be relatively thin and featureless, and the 120 CPs form a "$T=2$" icosahedral lattice. Segmentation of the capsid portion of the HvV190S cryo-reconstruction made it possible to assign all density features to either an "A" or a "B" subunit, labeled

according to the distinct locations they occupy in the icosahedron. Hence, the asymmetric unit of the icosahedron is an AB dimer, which consists of two chemically identical monomers.

ACKNOWLEDGMENTS

This work was supported in part by Kentucky Science and Engineering Foundation grant KSEF-2178-RDE-013 (S. A. G.) and by NIH grants R37-GM033050 and 1S10-RR020016 as well as UCSD and the Agouron Foundation (T. S. B.).

REFERENCES

Amrani, N., Ganesan, R., Kervestin, S., Mangus, D. A., Ghosh, S., & Jacobson, A. (2004). A *faux* 3' -UTR promotes mRNA decay. *Nature*, *432*, 112–118.

Bontems, F., Roumestand, C., Gilquin, B., Ménez, A., & Toma, F. (1991). Refined structure of charybdotoxin: Common motifs in scorpion toxins and insect defensins. *Science*, *25*, 1521–1523.

Bourges, N., Groppi, A., Barreau, B., Clave, C., & Begueret, J. (1998). Regulation of gene expression during the vegetative incompatibility reaction in *Podospora anserina*: Characterization of three induced genes. *Genetics*, *150*, 633–641.

Bruenn, J. (2004). The *Ustilago maydis* killer toxins. *Topics in Current Genetics*, *11*, 157–174.

Bryant, N. J., & Boyd, A. (1993). Immunoisolation of Kex2-containing organelles from yeast demonstrates co-localisation of three processing proteinases to a single Golgi compartment. *Journal of Cell Science*, *106*, 815–822.

Castón, R. J., Luque, D., Trus, B. L., Rivas, G., Alfonso, C., González, J. M., et al. (2006). Three-dimensional structure and stoichiometry of Helminthosporium victoriae 190S totivirus. *Virology*, *347*, 323–332.

Castón, J. R., Trus, B. L., Booy, F. P., Wickner, R. B., Wall, J. S., & Steven, A. C. (1997). Structure of L-A virus: A specialized compartment for the transcription and replication of double-stranded RNA. *The Journal of Cell Biology*, *138*, 975–985.

Covelli, L., Coutts, R. H. A., Di Serio, F., Citir, A., Acikgoz, S., Hernandez, C., et al. (2004). Cherry chlorotic rusty spot and Amasya cherry diseases are associated with a complex pattern of mycoviral-like double-stranded RNAs. I. Characterization of a new species in the genus Chrysovirus. *Journal of General Virology*, *85*, 3389–3397.

Dauplais, M., Lecoq, A., Song, J., Cotton, J., Jamin, N., Gilquin, B., et al. (1997). On the convergent evolution of animal toxins. *The Journal of Biological Chemistry*, *272*, 4302–4309.

de Sá, P. B., Havens, W. M., & Ghabrial, S. A. (2010). Characterization of a novel broad-spectrum antifungal protein from virus-infected *Helminthosporium* (*Cochliobolus*) *victoriae*. *Phytopathology*, *100*, 880–889.

de Sá, P. B., Li, H., Havens, W. M., Farman, M. L., & Ghabrial, S. A. (2010). Overexpression of the victoriocin gene in *Helminthosporium victoriae* enhances the antifungal activity of culture filtrates. *Phytopathology*, *100*, 890–896.

Dinman, J. D., Icho, T., & Wickner, R. B. (1991). A -1 ribosomal frameshift in a double-stranded RNA virus of yeast forms a gag-pol fusion protein. *Proceedings of the National Academy of Sciences of the United States of America*, *88*, 174–178.

Dinman, J. D., & Wickner, R. B. (1992). Ribosomal frameshifting efficiency and gag/gag-pol ratio are critical for yeast M1 double-stranded RNA virus propagation. *Journal of Virology*, *66*, 3669–3676.

Dreher, T. W., & Miller, W. A. (2006). Translational control in positive strand RNA plant viruses. *Virology*, *344*, 185–197.

Dunn, S. E., Li, H., Cardone, G., Nibert, M. L., Ghabrial, S. A., & Baker, T. S. (2013). Three-dimensional structure of victorivirus HvV190S suggests that the coat proteins in all totiviruses may share a conserved core. PLoS Pathogens (in press).

Fraga, J. S., Katsuyama, A. M., Fernandez, S., Madeira, A. M. B. N., Briones, M. R. S., & Gruber, A. (2006). The genome of the Eimeria brunetti RNA virus 1 is more closely related to fungal than to protozoan viruses. GenBank Accession No. AF356189. Unpublished

Gallie, D. R., & Walbot, V. (1992). Identification of the motifs within the tobacco mosaic virus 5'-leader responsible for enhancing translation. *Nucleic Acids Research*, *20*, 4631–4638.

Ghabrial, S. A. (1986). A transmissible disease of *Helminthosporium victoriae*: Evidence for a viral etiology. In K. W. Buck (Ed.), *Fungal virology* (pp. 353–369). Boca Raton: CRC Press.

Ghabrial, S. A. (2008a). Chrysoviruses. In B. W. J. Mahy & M. H. V. Van Regenmortel (Eds.), (3rd ed.). *Encyclopedia of virology*, vol. 1, (pp. 503–513). Oxford: Elsevier.

Ghabrial, S. A. (2008b). Totiviruses. In B. W. J. Mahy & M. H. V. Van Regenmortel (Eds.), (3rd ed.). *Encyclopedia of virology*, vol. 5, (pp. 163–174). Oxford: Elsevier.

Ghabrial, S. A., Bibb, J. A., Price, K. H., Havens, W. M., & Lesnaw, J. A. (1987). The capsid polypeptides of the 190S virus of *Helminthosporium victoriae*. *Journal of General Virology*, *68*, 1791–1800.

Ghabrial, S. A., & Havens, W. M. (1989). Conservative transcription of *Helminthosporium victoriae* 190*S* virus dsRNA *in vitro*. *Journal of General Virology*, *70*, 1025–1035.

Ghabrial, S. A., & Havens, W. M. (1992). The *Helminthosporium victoriae* 190*S* mycovirus has two forms distinguishable by capsid protein composition and phosphorylation state. *Virology*, *188*, 657–665.

Ghabrial, S. A., & Havens, W. M. (2013). Characterization of the protein kinase activity of the multifunctional protein Hv-p68 from Helminthosporium victoriae. Unpublished manuscript.

Ghabrial, S. A., Havens, W. M., Xie, J., & Annamalai P. (2013). Molecular characterization of the chrysovirus Helminthosporium victoriae virus 145S. Submitted manuscript.

Ghabrial, S. A., & Mernaugh, R. L. (1983). Biology and transmission of *Helminthosporium victoriae* mycoviruses. In R. W. Compans & D. H. L. Bishop (Eds.), *Double-stranded RNA viruses* (p. 441). New York: Elsevier.

Ghabrial, S. A., & Nibert, M. L. (2009). *Victorivirus*, a new genus of fungal viruses in the family *Totiviridae*. *Archives of Virology*, *154*, 373–379.

Ghabrial, S. A., & Pirone, T. P. (1967). Physiology of tobacco etch virus-induced wilt of Tabasco peppers. *Virology*, *31*, 154–162.

Ghabrial, S. A., Sanderlin, R. S., & Calvert, L. A. (1979). Morphology and virus content of *Helminthosporium victoriae* colonies regenerated from protoplasts of normal and diseased isolates. *Phytopathology*, *69*, 312–315.

Ghabrial, S. A., Soldevila, A. I., & Havens, W. M. (2002). Molecular genetics of the viruses infecting the plant pathogenic fungus *Helminthosporium victoriae*. In S. Tavantzis (Ed.), *Molecular biology of double-stranded RNA: Concepts and applications in agriculture, forestry and medicine* (pp. 213–236). Boca Raton, FL: CRC Press.

Ghabrial, S., & Suzuki, N. (2009). Viruses of plant pathogenic fungi. *Annual Review of Phytopathology*, *47*, 353–384.

Guo, L. H., Sun, L., Chiba, S., Araki, H., & Suzuki, N. (2009). Coupled termination/reinitiation for translation of the downstream open reading frame B of the prototypic hypovirus CHV1 EP713. *Nucleic Acids Research*, *37*, 3645–3659.

Hellen, C. U., & Sarnow, P. (2001). Internal ribosome entry sites in eukaryotic mRNA molecules. *Genes & Development*, *15*, 1593–1612.

Herrero, N., & Zabalgogeazcoa, I. (2011). Mycoviruses infecting the endophytic and entomopathogenic fungus Tolypocladium cylindrosporum. *Virus Research*, *160*, 409–413.

Huang, S., & Ghabrial, S. A. (1996). Organization and expression of the double-stranded RNA genome of Helminthosporium victoriae 190S virus, a totivirus infecting a plant pathogenic filamentous fungus. *Proceedings of the National Academy of Sciences of the United States of America*, *93*, 12541–12546.

Huang, S., Soldevila, A. I., Webb, B. A., & Ghabrial, S. A. (1997). Expression, assembly and proteolytic processing of *Helminthosporium victoriae* 190S totivirus capsid protein in insect cells. *Virology*, *234*, 130–137.

Jiang, D., & Ghabrial, S. A. (2004). Molecular characterization of Penicillium chrysogenum virus: Reconsideration of the taxonomy of the genus *Chrysovirus*. *Journal of General Virology*, *85*, 2111–2121.

Kozak, M. (2002). Pushing the limits of the scanning mechanism for initiation of translation. *Gene*, *299*, 1–34.

Li, H., Havens, W. M., Xie, J., & Ghabrial, S. A. (2013). Transformation of virus-free Helminthosporium victoriae with a full-length cDNA clone of HvV190S-CP confers a disease phenotype. Unsubmitted manuscript.

Li, H., Havens, W. M., Nibert, M. L., & Ghabrial, S. A. (2011). RNA sequence determinants of a coupled termination-reinitiation strategy for downstream open reading frame translation in *Helminthosporium victoriae* virus 190S and other victoriviruses (Family *Totiviridae*). *Journal of Virology*, *85*, 7343–7352.

Lindberg, G. D. (1959). A transmissible disease of *Helminthosporium victoriae*. *Phytopathology*, *49*, 29–32.

Lindberg, G. D. (1960). Reduction in pathogenicity and toxin production in diseased Helminthosporium victoriae. *Phytopathology*, *50*, 457.

Litzenberger, S. C. (1949). Nature of susceptibility to *Helminthosporium victoriae* and resistance to *Puccinia coronata* in Victoria oats. *Phytopathology*, *39*, 300–318.

Luttermann, C., & Meyers, G. (2007). A bipartite sequence motif induces translation reinitiation in feline calicivirus RNA. *The Journal of Biological Chemistry*, *282*, 7056–7065.

Luttermann, C., & Meyers, G. (2009). The importance of inter- and intramolecular base pairing for translation reinitiation on a eukaryotic bicistronic mRNA. *Genes & Development*, *23*, 331–344.

Matassova, N. B., Venjaminova, A. G., & Karpova, G. G. (1998). Nucleotides of 18S rRNA surrounding mRNA at the decoding site of translating human ribosome as revealed from the cross-linking data. *Biochimica et Biophysica Acta*, *1397*, 231–239.

Meehan, F., & Murphy, H. C. (1946). A new Helminthosporium blight of oats. *Science*, *104*, 413–414.

Meehan, F., & Murphy, H. C. (1947). Differential phytotoxicity of metabolic by-products of *Helminthosporium victoriae*. *Science*, *106*, 270–271.

Melin, P., Schnuürer, J., & Wagner, E. G. H. (2002). Proteome analysis of *Aspergillus nidulans* reveals proteins associated with the response of the antibiotic concanamycin A, produced by Streptomyces species. *Molecular Genetics and Genomics*, *267*, 695–702.

Melin, P., Schnuürer, J., & Wagner, E. G. H. (2003). Characterization of *phiA*, a gene essential for phialide development in *Aspergillus nidulans*. *Fungal Genetics and Biology*, *40*, 234–241.

Meyers, G. (2003). Translation of the minor capsid protein of a calicivirus isinitiated by a novel termination-dependent reinitiation mechanism. *The Journal of Biological Chemistry*, *278*, 34051–34060.

Meyers, G. (2007). Characterization of the sequence element directing translation reinitiation in RNA of the calicivirus rabbit hemorrhagic disease virus. *Journal of Virology*, *81*, 9623–9632.

Naitow, H., Tang, J., Canady, M., Wickner, R. B., & Johnson, J. E. (2002). L-A virus at 3.4 Å resolution reveals particle architecture and mRNA decapping mechanism. *Nature Structural Biology*, *9*, 725–728.

Nomura, K., Osahki, H., Iwanami, T., Matsumoto, N., & Ohtsu, Y. (2003). Cloning and characterization of a totivirus double-stranded RNA from the plant pathogenic fungus, *Helicobasidium mompa* Tanaka. *Virus Genes*, *26*, 219–226.

Ochoa, W. F., Havens, W. M., Sinkovits, R. S., Nibert, M. L., Ghabrial, S. A., & Baker, T. S. (2008). Partitivirus structure reveals a 120-subunit, helix-rich capsid with distinctive surface arches formed by quasisymmetric coat-protein dimers. *Structure*, *16*, 776–786.

Pan, J., Dong, L., Lin, L., Ochoa, W. F., Sinkovits, R. S., Havens, W. M., et al. (2009). Atomic structure reveals the unique capsid organization of a dsRNA virus. *Proceedings of the National Academy of Sciences of the United States of America*, *106*, 4225–4230.

Plant, E. W., Jacobs, K. M., Harger, J. W., Meskauskas, A., Jacobs, J. L., Baxter, J. L., et al. (2003). The 9-Å solution: How mRNA pseudoknots promote efficient programmed -1 ribosomal frameshifting. *RNA*, *9*, 168–174.

Powell, M. L., Brown, T. D., & Brierley, I. (2008). Translational terminationre-initiation in viral systems. *Biochemical Society Transactions*, *36*, 717–722.

Pöyry, T. A., Kaminski, A., Connell, E. J., Fraser, C. S., & Jackson, R. J. (2007). The mechanism of an exceptional case of reinitiation after translationof a long ORF reveals why such events do not generally occur in mammalian mRNA translation. *Genes & Development*, *21*, 3149–3162.

Psarros, E. E., & Lindberg, G. D. (1962). Morphology and respiration of diseased and normal Helminthosporium victoriae. *Phytopathology*, *52*, 693.

Reid, M. F., & Fewson, C. A. (1994). Molecular characterization of microbial alcohol dehydrogenases. *Critical Reviews in Microbiology*, *20*, 13–56.

Rockwell, N. C., & Fuller, R. S. (1998). Interplay between S1 and S4 subsites in the Kex2 protease: Kex2 exhibits dual specificity for the P4 side chain. *Biochemistry*, *37*, 3386–3391.

Ryabova, L. A., & Hohn, T. (2000). Ribosome shunting in the cauliflower mosaic virus 35S RNA leader is a special case of reinitiation of translation functioning in plant and animal systems. *Genes & Development*, *14*, 817–829.

Sanderlin, R. S., & Ghabrial, S. A. (1978). Physicochemical properties of two distinct types of virus-like particles from *Helminthosporium victoriae*. *Virology*, *87*, 142–151.

Sasaki, A., Kanematsu, S., Onoue, M., Oyama, Y., & Yoshida, K. (2006). Infection of *Rosellinia necatrix* with purified viral particles of a member of *Partitiviridae* (RnPV1-W8). *Archives of Virology*, *151*, 697–707.

Scheffer, R. P., & Nelson, R. R. (1967). Geographical distribution and prevalence of Helminthosporium victoriae. *The Plant Disease Reporter*, *51*, 110.

Schmitt, M. J., & Breinig, F. (2006). Yeast viral killer toxins: Lethality and self-protection. *Nature Reviews Microbiology*, *4*, 212–221.

Schoch, C. L., Shoemaker, R. A., Seifert, K. A., Hamleton, S., Spatafora, J. W., & Crous, P. W. (2006). A multigene phylogeny of the Dothideomycetes using four nuclear loci. *Mycologia*, *98*, 1041–1052.

Soldevila, A. I., & Ghabrial, S. A. (2000). Expression of the totivirus *Helminthosporium victoriae 190S Virus* RNA-dependent RNA polymerase from its downstream open reading frame in dicistronic constructs. *Journal of Virology*, *74*, 997.

Soldevila, A. I., & Ghabrial, S. A. (2001). A novel alcohol oxidase/RNAbinding protein with affinity for mycovirus double-stranded RNA from the filamentous fungus *Helminthosporium* (*Cochliobolus*) *victoriae*. *The Journal of Biological Chemistry*, *276*, 4652–4661.

Soldevila, A. I., Huang, S., & Ghabrial, S. A. (1998). Assembly of the Hv190S totivirus capsid is independent of posttranslational modification of the capsid protein. *Virology*, *251*, 327–333.

Soldevila, A., Havens, W. M., & Ghabrial, S. A. (2000). A cellular protein with RNA-binding activity co-purifies with viral dsRNA from mycovirus infected *Helminthosporium victoriae*. *Virology*, *272*, 183–190.

Tang, J., Ochoa, W. F., Sinkovits, R. S., Poulos, B. T., Ghabrial, S. A., Lightner, D. V., et al. (2008). Infectious myonecrosis virus has a totivirus-like, 120-subunit capsid, but with fiber complexes at the fivefold axes. *Proceedings of the National Academy of Sciences of the United States of America*, *105*, 17526–17531.

Tang, J., Ochoa, W. F., et al. (2010). Structure of Fusarium poae virus 1 shows conserved and variable elements of partitivirus capsids and evolutionary relationships to picobirnavirus. *Journal of Structural Biology*, *172*, 363–371.

Wang, A. L., Yang, H. M., Shen, K. A., & Wang, C. C. (1993). Giardiavirus double-stranded RNA genome encodes a capsid polypeptide and a gag-pol like fusion protein by a translation frameshift. *Proceedings of the National Academy of Sciences of the United States of America*, *90*, 8595–8599.

Weiler, F., & Schmitt, M. J. (2005). Zygocin—a monomeric protein toxin secreted by virus infected Zygosaccharomyces bailli. *Topics in Current Genetics*, *11*, 175–187.

Wheeler, H., & Black, H. S. (1962). Change in permeability induced by victorin. *Science*, *137*, 983–984.

Wickner, R. B. (1996). Double-stranded RNA viruses of Saccharomyces cerevisiae. *Microbiological Reviews*, *60*, 250–265.

Wolpert, T. J., Macko, V., Acklin, W., Jaun, B., Seibl, J., Meili, J., et al. (1985). Structure of victorin C, the major hostselective toxin from *Cochliobolus victoriae*. *Experientia*, *41*, 1524–1529.

Xie, J., & Ghabrial, S. A. (2013). Molecular characterization of the P30 gene encoding a cell wall protein overexpressed in virus-infected Helminthosporium victoriae. Unpublished manuscript.

Yount, N. Y., & Yeaman, M. R. (2004). Multidimensional signatures in antimicrobial peptides. *Proceedings of the National Academy of Sciences of the United States of America*, *101*, 7363–7368.

Zapf, M. W., Theisen, S., Rohde, S., Rabenstein, F., Vogel, R. F., & Niessen, L. (2007). Characterization of AfpA, an alkaline foam protein from cultures of *Fusarium culmorum* and its identification in infected malt. *Journal of Applied Microbiology*, *103*, 36–52.

Zhao, T., Havens, W. M., & Ghabrial, S. A. (2006). Disease phenotype of virus-infected *Helminthosporium victoriae* is independent of overexpression of the cellular alcohol oxidase/RNA binding protein Hv-p68. *Phytopathology*, *96*, 326–332.